Ethernet-over-SDH: Technologies Review and Performance Evaluation

Antônio Marcos Alberti & Roulien Fernandes

***Abstract*— The Generic Framing Procedure, Virtual Concatenation and the Link Capacity Adjusting Scheme are successful technologies that brought new life to synchronous networks. They facilitated efficient, flexible and robust interconnection of two of the most deployed technologies ever: Ethernet and *Synchronous Digital Hierarchy* (SDH). The objective of this tutorial is to present an overview of these *Ethernet-over-SDH* (EoS) technologies, focusing on their performances. We reviewed literature from 2001-2009 and present the main aspects of EoS technologies and performance as well as notable formulations for EoS throughput, efficiency and delay. We reviewed the fundamental evolution steps of both Ethernet and SDH. The paper also covers experimental methodology and scenario configuration for EoS performance evaluation in the laboratory, discusses measured results and compares the presented analytical expressions and calculations with experimental data. An in-depth performance evaluation of EoS networks is conducted.**

***Index Terms*— Performance, Evaluation, SDH, GFP, LCAS, VCat**

1. Introduction

Ethernet [1] and SDH [2] are landmark technologies for computer and telecommunications networking, respectively. However, digital network convergence has pushed both to work together. This demand drove the creation of a set of new technologies to efficiently and flexibly combine both worlds. The *Generic Framing Procedure* (GFP) [3] provides several functions to adapt Ethernet traffic to transportation in SDH networks. *Virtual Concatenation* (VCat) [2] allows the separation of GFP-adapted traffic into different paths in an SDH network. The *Link Capacity Adjustment Scheme* (LCAS) [4] dynamically adjusts the capacities of SDH paths according to source and/or destination needs. In combination, these technologies have brought new life to SDH. In fact, this new network vision was named *Next Generation SDH* (NG-SDH). Ethernet exhibits all its advantages when combined with NG-SDH, not only in terms of flexibility and simplicity, but also in terms of cost and capacity. This convergent network was fully adopted by telcos in metropolitan and long-distance areas. Many operators bought expansion cards for their SDH equipment to allow encapsulation and mapping of Ethernet traffic to SDH.

Despite the importance of such technologies and their interplay, the literature lacks a general overview of EoS technologies that includes performance evaluation. We believe that the topics addressed in this paper are of practical and tutorial value, specially considering the overspread presence of EoS networks. Therefore, this paper focuses on description, discussion and performance evaluation of EoS technologies. The remainder of the paper is organized as follows: Section 2 presents a technology overview including Ethernet, SDH, EoS, GFP, VCat and LCAS; Section 3 describes previous work related to EoS and evaluating its performance; Section 4 presents an analytical treatment of throughput, efficiency and delay in EoS networks. This is another contribution of the paper. Section 5 describes the methodology used in an experimental performance evaluation of EoS done at Telefonica laboratories, Brazil. Five scenarios were examined in a controlled testbed, and the corresponding throughput, efficiency and delay are presented, discussed and compared with analytical results. GFP, VCat and LCAS protocols were tested using a standardized methodology; finally, in Section 6 we conclude with some final remarks.

Manuscript received in February 3, 2011; revised in .

A. M. Alberti (alberti@inatel.br) is with Instituto Nacional de Telecomunicações - Inatel. Av. João de Camargo, 510 - Santa Rita do Sapucaí - MG - Brasil - 37540-000.

R. Fernandes (rfernand@telefonica.br) is with Telefonica S.A., São Paulo, SP, Brazil.

2. Technology Overview

A. Ethernet

Ethernet is a connectionless packet-switching technology, defined by a set of physical and data link specifications, functions and protocols originally developed for computer networking. According to Spurgeon [5], Ethernet arose in 1973, when Bob Metcalfe wrote a memo describing a network technology to connect computer work stations. In 1976, Bob Metcalfe and David Boggs published a paper to describe Ethernet [1]. The first Ethernet standard was published in 1980 by the DEC-Intel-Xerox (DIX) consortium [6]. In 1985, the 802.3 standardization committee of the *Institute of Electrical and Electronics Engineers* (IEEE) published its Ethernet standard with the title *IEEE 802.3 Carrier Sense Multiple Access with Collision Detection (CSMA/CD) Access Method and Physical Layer Specifications* [7]. This standard specified operation at 10 Mbits/s. The CSMA/CD technique was proposed to control multiple stations access to a coaxial cable diffusion media, forming a physical bus. Since 1985, a set of standards emerged for new media, speeds and other features. A complete list of IEEE 802.3 standards can be found in [7].

Today, Ethernet is the dominant technology in computer *Local Area Networks* (LANs) [5], [8], [9]. Ethernet standard IEEE 10BASE-T [7] provided up to 10 Mbit/s in one unshielded twisted pair using baseband Manchester line coding [9]. The maximum segment size is 100 meters. The 10BASE-T standard became widely adopted to transport *Internet Protocol* (IP) [10] datagrams, which are accommodated on Ethernet frames. An Ethernet frame contains [7]: a 7-octet *Preamble*,

which is a sequence of alternated 0s and 1s used to establish bit synchronization between source and destination hardware; a 1-octet *Start-of-Frame-Delimiter* (SFD), which indicates the first bit of the rest of the frame; 12 octets of *Source* and Destination *Media Access Control* (MAC) data link sublayer addresses; a 2-octet *Length/Type* that takes one of two meanings: to indicate frame length in IEEE 802.3 standards (which is limited to 1518 octets), or to indicate which network layer protocol is being carried in the frame, in order to maintain compatibility with the DIX standard; 46 to 1500 octets of MAC client data and/or padding; and 4 octets of *Frame Check Sequence* (FCS) which is a 32-bit *Cyclic Redundancy Check* (CRC). For the CSMA/CD protocol to function correctly, a minimum MAC frame size is required, and thus padding can be added to the frame if needed.

Also, IEEE 802.3 [7] defines an *Inter-Packet Gap* (IGP) between Ethernet frames to provide adequate recovery times for procedures in the link and physical layers, such as cycling circuitry from transmit to receive mode in half-duplex operation. The IGP for 10BASE-T standard is 9.6 μ seconds, while it is 0.96 μs for 100BASE-T. This is equivalent to 12 bytes of emission time in these standards. The IGP is related to the *Inter-Frame Spacing* (IFS). According to [11], the IFS is the sum of at least 12 bytes of IGP, plus a 7-octet *Preamble* and a 1-octet SFD. Also, Ramamurti et al. [12] discusses IFS and IGP, and IGP use for rate adaptation in EoS.

In July 1995, IEEE standard 802.3u was officially approved, creating what became known as *Fast Ethernet* [13]. Fast Ethernet refers to a compatible IEEE 802.3 standard operating at 100 Mbit/s. According to Tanenbaum [14], all Fast Ethernet standards were based on hubs, switches, twisted pairs and fiberoptics; coaxial cables were not allowed. For example, Ethernet IEEE 100BASE-T [7] uses two twisted pairs with a maximum segment length of 100 meters. Note that the Ethernet frame remained the same as in 10BASE-T. With 100 Mbit/s available to the user stations, even higher data rates become necessary in servers and high capacity links.

Gigabit Ethernet (GbE) was developed to interconnect 10/100 Mbit/s switches and to provide higher data rates. The Gigabit Ethernet standardization effort started with the IEEE 802.3z [15] standard in 1996, and industrial interest in this technology led to the creation of the Gigabit Ethernet Alliance, which was organized to facilitate and accelerate the introduction of this technology into the market. GbE defined support for single-mode optical fiber (1000BASE-LX), greatly increasing network reachability.

In 2002, Ethernet standard IEEE Std 802.3ae-2002 introduced 10 Gigabit Ethernet (10GbE) [16], [17]. The goal of 10 GbE was to cover distances from 300 meters to 40 km. Only optical physical layer options were defined. In addition, 10 GbE does not support half- duplex operation or CSMA/CD; all operation is in full-duplex mode.

The scalability, simplicity and cost effectiveness of Ethernet, along with its high rates and optical network support, led many service providers to consider Ethernet in *Metropolitan Area Networks* (MANs) and *Wide Area Networks* (WANs), where it is referred to as *Metro Ethernet* [18]. Ethernet scalability means that the quantity of equipment can be dramatically extended, and the network continues to operate adequately.

Simplicity means that the network is relatively simple when compared with other link layer technologies, like *Asynchronous Transfer Mode* (ATM) [19] and *Synchronous Digital Hierarchy* (SDH) [2]. Self-negotiation, introduced in IEEE 802.3u, also simplifies network usage and operation. Also, Ethernet operation is similar at any rate or scale.

According to Brockners et al. [18], with these advantages Ethernet became the de facto MAN technology, allowing seamless, flexible and reliable interconnection of LANs using a single high-speed network technology. To address the technological and architectural challenges behind Metro Ethernet [20], standardization bodies like the IEEE, *Internet Engineering Task Force* (IETF) and *International Telecommunication Union - Telecommunication Standardization Sector* (ITU-T) developed several standards dedicated to facilitating new and innovative Ethernet-based communication services. Also, *Metro Ethernet Forum* (MEF) was founded in 2001 to promote worldwide adoption, interoperability and deployment of carrier-class Ethernet networks and services in traditional service providers. These efforts led to a new class of Ethernet that is being called *Carrier Ethernet* [21]–[24].

MEF defines Carrier Ethernet as "*A ubiquitous, standardized, carrier-class Service and Network defined by five attributes that distinguish it from familiar LAN-based Ethernet: Standardized Services, Scalability, Service Management, Reliability and Quality of Service (QoS).*" [24]. Ubiquitous means that this type of Ethernet will be omnipresent, from enterprise and home broadband arenas to long-distance backbones. Carrier-class services means services of a quality equivalent to that offered by traditional service providers. Service standardization means to standardize services in order to precisely describe them in *Service Level Agreements* (SLAs), which are the agreements between the end user and the network. However, the evolution of LAN Ethernet towards Carrier Ethernet requires that several challenges be addressed [20].

Regarding service standardization, MEF, ITU-T and IETF have been working on the definition of frameworks to support some innovative services in Ethernet. ITU-T defined a services framework in Recommendation G.8011 [26], and MEF described a framework in MEF6.1 [27]. Both frameworks are based on the establishment of *Ethernet Virtual Connections* (or *Circuits*) (EVCs) among two or more *User-to-Network Interfaces* (UNIs). An EVC allows the transfer of Ethernet frames among the UNIs that belong to it and prevents the transfer of frames from other UNIs. EVCs could be point-to-point, multipoint-to-multipoint or rooted multipoint. Point-to-point EVC means that the EVC is created between two UNIs. Multipoint-to-multipoint EVCs can associate more than two UNIs. Therefore, Ethernet frames that enter at one UNI can be replicated in such a way that copies are delivered to other participating UNIs. A rooted-multipoint EVC is more complicated. It separates UNIs into roots and leaves. Traffic entering at a root UNI can be sent to any or all of the other UNIs. However, traffic entering from leaf UNIs could be transferred to one or more root UNIs, but never to other leaf UNIs. This provides traffic isolation among the leaves. EVCs could also be bundled, meaning that multiple VLANs

could use the same EVC.

ITU-T defined two EVC services [26]: *Ethernet Private Line* (EPL) and *Ethernet Virtual Private Line* (EVPL); and two more are under development: *Ethernet Virtual Private LAN* (EVPLAN) and Ethernet TREE. MEF defined three service types in its Ethernet Services Definition Specification [27]: *E-Line*, *E-LAN* and *E-Tree*, which generate six derived services. IETF defined *Virtual Private LAN Service* (VPLS) in RFC 4762 [28]. Generally speaking, line services are point-to-point services created to replace TDM private lines, ATM and Frame Relay services, while LAN services are focused on transparent or private VLAN services. Some comparison of ITU-T and MEF standards for Ethernet services were provided in the appendices of ITU-T Recommendations [26].

IEEE standard IEEE802.1Q-2005 [29] standardized VLANs, which are sometimes called *virtual bridged networks*. The idea is to separate logical connectivity from physical connectivity, allowing applications/users to view the network without being limited by the physical topology [30]. In other words, the LAN is virtual because it can be extended beyond a certain physical LAN, and the traffic is separated in such a way that it appears to be in the same LAN. Each IEEE 802.1Q Tagged Ethernet frame receives a *Tag Control Information* (TCI) field [29] with 12 bits reserved for VLAN identification, which is frequently called the Q-tag. This means that 4094 VLANs can be created in an organization network. When VLANs are extended to the domains of more than one organization, the Q-tag overlap problem appears. IEEE 802.1ad [31] and IEEE 802.1ah [32] proposed solutions to this problem. For more details, see Sanchez et al. [22].

According to Xiao [33], Ethernet QoS was first improved in 1998, when IEEE 802.1p was published as a part of the IEEE 802.1D standard [34]. Each IEEE 802.1Q Tagged Ethernet frame receives a 3-bit *Priority Code Point* (PCP) field to support 8 traffic classes and provide service differentiation in the LAN [29]. Ethernet QoS and Traffic Management are being studied by ITU-T, MEF and IEEE. The recent ITU-T Recommendations Y.2112 specifies a QoS control architecture for Ethernet-based IP access networks [35]. MEF specification 10.1 [36] covers performance parameters for services and QoS control. IEEE 802.1Qay [37] addresses *Provider Backbone Bridge Traffic Engineering* (PPB-TE), introducing a connection-oriented forwarding mode for Ethernet.

Ethernet also could be used to provide first-mile access. *Ethernet Passive Optical Network* (EPON) was standardized by IEEE Std. 802.3ah-2004 [38]. Briefly, it uses two wavelengths in a single fiberoptic cable to transport full-duplex Ethernet frames. Passive optical elements are used to separate traffic from backbone to each Ethernet terminal. Please refer to Mukherjee [39] for more details on EPON.

According to Ohta [25], Ethernet enhancements are being standardized in the following areas: "*High-bit-rate and long-distance interfaces; Capability enhancements as access networks; Virtual Local Area Network (VLAN) scalability enhancement; Operation, Administration, and Maintenance (OAM); Fast survivability; Handling of realtime signals; and Traffic engineering*." The work for the 100 Gbit/s standard has already begun in the IEEE 40Gb/s and 100 Gbit/s Ethernet Task Forces. The formal designation for this standard will be IEEE 802.3ba. To deal with of the high diversity of Ethernet services in multidomain networks, scalability is being addressed by IEEE 802.1ad [31] and IEEE 802.1ah [32]. OAM was improved in IEEE 802.1ag [40] and ITU-T Recommendation Y.1731 [41]. Fast survivability technologies were proposed in ITU-T Recommendation G.8031 [42] and IEEE 802.1Qay [37]. Another initiative is the Generalized Multiprotocol Label Switching (GMPLS) Controlled Ethernet Label Switching (GELS) [81], which aims to control Ethernet switches using GMPLS.

In the next section, we will briefly present SDH, and we will discuss Ethernet-over-SDH transport in Section 23

B. Synchronous Digital Hierarchy (SDH)

SDH [2] is a hierarchy of synchronized digital TDM structures that relies on circuit switching to establish dedicated electronic-optical-electronic paths through the network. It is defined by a set of physical and data link specifications, functions and protocols originally developed for telephone networking. Synchronous operation means that TDM structures are synchronized by a complex time-space synchronization network, based on sophisticated time reference standards. Such structures are hierarchical in the sense that multiple lower-rate structures could be time-multiplexed on higher-rate structures, which is known as the SDH multiplexing structure. The duration of the TDM frame is equal to 125 μseconds at all levels of the hierarchy. This value is the inverse of the voice sampling rate (8kHz) in traditional *Pulse Coded Modulation* (PCM). Each dedicated path receives a timeslot in one of the TDM structures, where digital content is transmitted as a continuous flow of bits in a totally different way than the packet storage technique used in packet-switched networks. This explains why time-space synchronization is necessary: the time adjustments that can be made on bit flows are very limited, and every octet must fit into the right timeslot.

In 1988, SDH was standardized by ITU-T in Recommendation G.707 [2]. SDH is very similar to *Synchronous Optical Network* (SONET) technology, which was proposed by BellCore (now Telcordia) and standardized by ANSI in 1985. Both SDH and SONET are widely deployed technologies, as they were adopted by virtually every telephone company in the world. SDH was developed to increase circuit-switched network capacity in the 90s, as former digital hierarchies, namely *Plesiochronous Digital Hierarchy* (PDH) and *Digital Carrier System*, were becoming limited in their abilities to support the growth in traffic demand. In addition, SDH operates quite well with *Wavelength Division Multiplexing* (WDM) technology, providing compatible carrier-class networks. In general, each WDM wavelength is used to provide transportation for one high-level SDH frame.

The latest revision of G.707 is from January 2007. It specifies SDH frame and multiplexing structures, bit rates, line interfaces, formats for mapping and multiplexing of client signals (e.g., PDH, ATM and Ethernet), elements and overheads into frames. The SDH client bit flow is accommodated in the payload area of a logical structure called the *Virtual Container*

(VC), which defines an end-to-end dedicated path for client content transportation. G.707 standardizes five VCs: VC-11, VC-12, VC-2, VC-3 and VC-4, with nominal rates of 1664 kbit/s, 2240 kbit/s, 6848 kbit/s, 48384 kbit/s and 150336 kbit/s, respectively. Each VC has a control subchannel called the *Path Overhead* (POH). Therefore, the available bit rate for client flow is slightly smaller than the rates quoted above.

The SDH multiplexing structure is based on three operations: *mapping*, *alignment* and *multiplexing*. The process of adjusting the tributary traffic rate to be accommodated in an SDH VC rate is called mapping. A mapped tributary data rate must have a nominal rate and an acceptable deviation around this value, otherwise desynchronization will occur. Limited deviations are accommodated by floating through pointers. Alignment is the process of rate adjusting between a VC and an intermediate transport structure, namely the *Tributary Unit* (TU), *Tributary Unit Group* (TUG), *Administrative Unit* (AU) and *Administrative Unit Group* (AUG). Alignment uses AU Pointers to allow a VC to float within the AU frame.

The SDH multiplexing structure allows ("nest") multiples VCs to be multiplexed in other high rate VCs or in an AUG. One AUG forms the *Synchronous Transport Module* (STM) level 1 or STM-1, which is the first level of the SDH hierarchy. AUGs can be multiplexed in multiples of 4 to form higher STM levels (STM-N) up to N=256, which has 39,813,120 kbit/s. The STM-N also have control channels called *Section Overhead* (SOH). Please refer to G.707 [2], Mukherjee [39] and Stallings [9] for more details about the multiplexing structure of SDH.

Recommendation G.707 defines mapping procedures for asynchronous and synchronous tributaries (defined in G.702 [43]), ATM cells, *High-Level Data Link Control* (HDLC) [44] frames and *Generic Framing Procedure* (GFP) frames, among others. ATM cell mapping is performed by aligning the byte structure of every cell with the VC byte structure in use. ATM cells can cross the container border, meaning that a cell may be partially transmitted in a certain VC time slot. GFP mapping does not require rate adaptation, as GFP frames arrive as a continuous byte stream with a capacity identical to the VC payload. HDLC mapping is very similar.

SDH provides two mechanisms to allow transportation of signals that do not fit efficiently into standardized VCs: *Contiguous Concatenation* (CCat) and *Virtual Concatenation* (VCat). CCat is a multiplexing mechanism that allows the concatenation of two or more VCs of the same rate to provide transport for payloads that require a greater capacity. A contiguous concatenated VC is referred to as VC-n-Xc, where n=12,11,2,3 or 4. Contiguously concatenated VCs remain multiplexed together during transportation over a single path in the network. All of the intermediate nodes need to identify the VC-n-Xc. VCat is an inverted multiplexing scheme where a high-capacity payload is demultiplexed into two or more VCs of the same data rate. A virtual concatenated VC is referred as VC-n-Xv, where n=12,11,2,3 or 4. Each individual VC of a VC-n-Xv can be transported over a different path in the network. Therefore, individual VCs must be multiplexed again to reassemble the original payload signal at the receiving end. VCat functionality need only be present at the path termination points. Notice that both concatenations provide the same data rate, which is $X*$ the VC-n data rate. Also, observe that standardized mappings include options to map signals not only for VCs, but also for VCs contiguously or virtually concatenated. VCat will be discussed in more detail in Subsection 2.E.

Regarding OAM and availability, SDH is a reference technology, as it was originally developed for carrier-grade WAN. Network operation is constantly monitored at different levels, from individual VCs to STMs. There are different OAM signals that indicate operational status, warnings and severe failures. POH and SOH are used to transport OAM information. SDH availability and survivability have been improved by robust protection and restoration mechanisms. A recent standard, G.784 [45], addresses SDH fault, configuration and performance management.

C. Ethernet-over-SDH

The original SDH traffic holds a nominal rate and an acceptable deviation around this value. VCs can be considered nearly constant in terms of bit rate. However, Ethernet traffic can vary from zero up to the nominal capacity of a link, i.e., it adjusts well to *Variable Bit Rate* (VBR) computer network traffic. The first approach to transport this VBR traffic over SDH was to allocate the closest VC that satisfies the data rate requirement, even if the client isn't using this data rate all of the time. Obviously, this solution could lead to under-utilization of SDH VCs. Another option could be to multiplex several Ethernet flows to fulfill the available VC payload, as discussed in Ethernet services. However, this solution could result in time periods with no traffic between LANs (or VLANs), for example. Therefore, it became evident that some internal SDH mechanism must be developed to allow dynamical adjusting of the allocated data rate. In 2004, ITU-T Recommendation G.7042/Y.1305 [4] specified a protocol to dynamically increase or decrease the available data rate in integer multiples of virtually concatenated VCs. This method is called *Link Capacity Adjustment Scheme* (LCAS) and allows the data rate to be dynamically adjusted without service interruption.

There was also the problem that the SDH data rate is allocated in large steps. For example, consider mapping Fast Ethernet MAC frames over SDH. This traffic should be mapped to a VC-4 with 149.760 Mbit/s of bulk net capacity, limiting utilization to 70%. The problem is even worse for Gigabit Ethernet. In this case, the traffic should be mapped to a VC-4-16c, that is, a VC-4 concatenated contiguously sixteen times, resulting in at most 42% utilization. VCat can deal with this problem better, because its inverted multiplexing scheme allows a contiguous data rate to be broken into individual low- or high-order VCs. Thus, a tributary can be mapped to a combination of VCs at the same rate that better fits the tributary's data rate requirements.

Although VCat and LCAS can improve VC payload utilization and adapt to the asynchronous nature of Ethernet, what happens if there aren't enough Ethernet frames in a certain instant of time to fulfill the available data rate in VC(s)?

Something must adequately fulfill the VC(s) payload, because SDH byte transmission is continuous. This problem is known as *rate adaptation*, and can occur even if an adequate number of VCs is designated to a certain Ethernet traffic stream.

Notice that Ethernet traffic can be individual MAC frames or *physical* (PHY) line coding. There is a great difference the bit rate of these two formats. For example, the physical line coding rate for a 100BASE-TX standard is 125 Mbit/s, while it is 1.25 Gbit/s for 1000BASE-LX. In these cases, the transmission of Ethernet physical line coding over SDH adds 25% overhead. According to Ramamurti [12], "*considerable bandwidth savings can be achieved if just the Ethernet frames are mapped into SONET*". However, the direct transport of Ethernet MAC frames over SDH is not possible, because SDH needs a balanced DC level (i.e., an equal number of 1s and 0s on average). According to Bernstein et al. [46], it was observed in initial deployments of Packet-over-SONET that certain bit patterns in packets could produce *Loss of Frame* (LOF) alarms in SONET. "*The problem was attributed to the relatively short period of the SONET section (SDH regenerator section) scrambler*". Therefore, additional scrambling is needed for Ethernet MAC frames. This explains why Ethernet frames are typically encapsulated in other protocols that perform scrambling before SDH mapping. To encapsulate means to create a *tunnel* to transport tributary traffic transparently over SDH.

The technological overview of encapsulation options for Ethernet-over-SDH was already addressed by other previous papers. In 1998, Manchester et al. [47] provided an overview on IP over SONET using PPP and HDLC. In 2001, Bonenfant and Rodriguez-Moral [48] presented a comprehensive overview of IP-over-fiber mappings, including Ethernet-over-SDH. Also, Scholten, Hernandez-Valencia and Zhu [49], [50] discussed encapsulation options in 2002. Figure 1 shows some possible EoS encapsulations.

One of the first encapsulation options for EoS was HDLC [44], which mainly provides frame delineation and scrambling. The HDLC frames are byte-aligned to the SDH VCs payload area, as standardized in Section 10.3 of G.707. Byte-aligned means that each HDLC character is aligned to the bytes of the VC. To adjust the asynchronous nature of HDLC frame arrival, an HDLC flag pattern (7Eh) is used to fill interframe spaces. HDLC uses a byte-stuffing technique to avoid false delineation that could occur when the payload is equal to the delimiter flags or escape characters. According to Li et al. [51], byte stuffing may increase frame length and unnecessarily reduce throughput. HDLC mapping includes also scrambling and descrambling procedures to balance the bit density.

Another option, similar to HDLC, is ITU-T Recommendation X.85/Y.1321: *Link Access Procedure for SDH* (LAPS) [52], standardized in 2001. LAPS is a simplified version of HDLC and is fully compatible with RFC 2615 [53], which defines PPP-over-SDH. Therefore, LAPS could be used to encapsulate IP traffic as well. Recommendation X.86/Y.1323 [54] defines how Ethernet frames are encapsulated over LAPS. After encapsulation, LAPS frames are mapped to SDH using the same procedure as HDLC. Scrambling and descrambling is provided for LAPS frames. A very useful comparison between LAPS and PPP/HDLC is provided in Appendix A of X.85 [52]. ATM can also be used by means of the *ATM Adaptation Layer* 5 (AAL5) protocol [48], but this option is quite inefficient, as it introduces too much overhead.

Finally, there is GFP [3], which according to Scholten et al. [50] "*overcomes the drawbacks of ATM and HDLC-based encapsulation*". GFP provides efficient and flexible encapsulation and mapping of both MAC and PHY Ethernet traffic. It fills the role of a protocol that is generic enough to encapsulate and efficiently map any type of signal to SDH.

D. Generic Framing Procedure (GFP)

GFP is a protocol developed to efficiently adapt traffic from several technologies to a bit/byte synchronous channel like SDH, *Optical Transport Network* (OTN) [55] or PDH. According to Hernandez-Valencia et al. [49], GFP standardization was a joint effort of the *American National Standards Institute* (ANSI) and ITU-T. GFP is standardized in ITU-T Recommendation G.7041/Y.1303 [3], from January 2001, but there is a more recent version from October 2008. The mapping of GFP frames to SDH is standardized in Recommendation G.707/Y.1322 [2], while the mapping to OTN is specified in ITU-T Rec. G.709/Y.1331. GFP was developed to improve equipment interoperability and to increase mapping performance with a low-complexity adaptation mechanism. The objective was to standardize mapping procedures to synchronous technologies.

GFP functionality is divided into client-dependent (client-specific) and client-independent (common to all clients) [49] functions. The client-independent functions are GFP frame delineation, data link synchronization, data link scrambling, client PDU multiplexing, client-independent performance monitoring and rate adaptation. The client-specific functions are mapping of client traffic in GFP payload and client-specific performance monitoring.

The GFP frame payload can be fulfilled with client technology frames or coded bit streams. The first option is *Protocol Data Unit* (PDU)-oriented and known as *GFP-Framed* (GFP-F) mode. It allows the adaptation of Ethernet MAC frames as well as *Multiprotocol Label Switching* (MPLS) [56], IP and *Point-to-Point Protocol* (PPP) [57] traffic. The second option is block-code-oriented, constant-bit-rate and known as *GFP-Transparent* (GFP-T) mode. In this case, bit streams such as Ethernet PHY, IBM *Enterprise Systems Connection* (ESCON) [58], *Fiber Connectivity* (FICON), or *Fiber Channel* [58] can fill the GFP frame payload. According to [59], in GFP-F client frames are received, processed and mapped in GFP frames, while in GFP-T the client block-coded characters are accommodated into GFP payload without the need to wait for an entire frame, thereby reducing packetization delay. No matter which option is being used, it is important to note that GFP hardware is implemented only in the edge equipment. Therefore, the legacy SDH core equipment remains unchanged. Scholten et al. [50] and Gorshe [60] discussed why GFP provides two modes of client traffic mapping. The answer is that each mode has unique benefits, therefore justifying standardization.

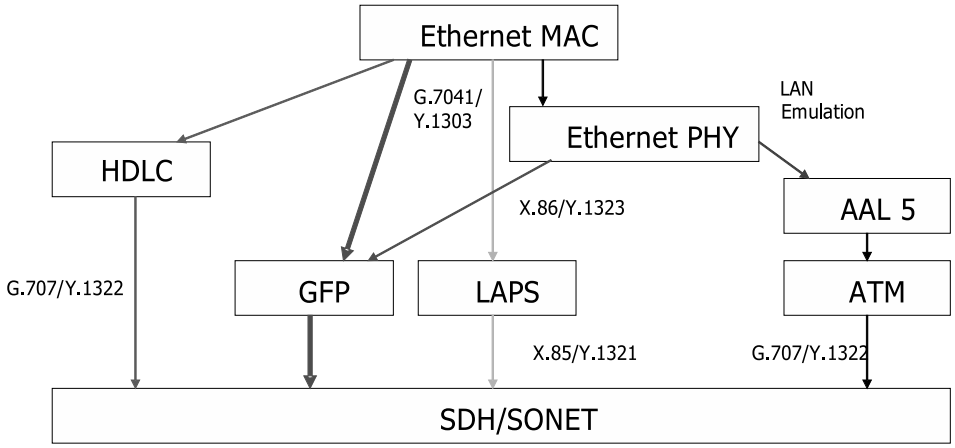

Fig. 1. Some options for encapsulating and mapping Ethernet traffic to SDH networks.

GFP frame delineation uses a *Header Error Check* (HEC) algorithm that is different from previously existing HDLC, PPP and LAPS bit/byte stuffing techniques, which introduce unnecessary inflation. This mechanism allows self-delineation, which means that frame delineation is achieved by successive successes in *Cyclic Redundancy Check* (CRC) calculations. The GFP receiver must successfully recognize frame boundaries, independent of the bit/byte alignment process used in SDH/SONET/OTN networks [49]. Scrambling is performed in the GFP frame header and payload to achieve high bit transition density. The same technique is used in both GFP-F and GFP-T modes.

GFP frames can accommodate fixed- or variable-size payloads. Fixed-size provides a TDM-like channel, while variable-size payloads allow a one-to-one mapping of client frames to GFP [49], dispensing with the segmentation and reassembly functions. If the client frames are absent, rate adaptation is done using *GFP Idle Frames*, which are four-octet long frames configured with null content. This facilitates rate adaptation of client signals to any transport medium with a higher capacity than the one required by the client signal. Statistical multiplexing could be used to share a single GFP link and better use the available virtual container rate. For example, the unidirectional traffic of an Ethernet Virtual Private LAN could be multiplexed together in just one GFP flow across an SDH network.

GFP provides *Client Signal Fail* (CSF) management. If a failure (or degradation) occurs in the input signal at the GFP source adaptation equipment, a CSF message will be sent to the destination equipment in time intervals from 100 ms to 1 second. *GFP Idle Frames* will be sent to the GFP sink adaptation equipment, in order to keep the line rate constant. When the GFP sink receives this failure indication, it declares a *Sink Client Signal Failure* (SCSF) [3], [50]. The CSF management allows the source to indicate the following types of failure [3], [49]: "*loss of client signal (e.g. loss of light) and loss of client character synchronization*". The defect condition at the far-end GFP sink remains until a valid GFP frame is received or if a certain number of CSF indications fail to be received.

A GFP frame is divided into two portions: *Core Header* and *Payload Area*, as shown in Figure 2. The core header contains a 2-octet *Payload Length Indicator* (PLI) and a 2-octet *Core Header Error Control* (cHEC), which is a CRC-16 code used to protect the Core Header. The payload area is subdivided into three portions: *Payload Area Header*, *Client Payload Information* and *Optional Payload Frame Check Sequence*, which is an optional CRC code with 32 bits. There two types of GFP frames: client frames and control frames. Control frames are identified by PLI values in the range from 0 to 3, while client frames have PLI equal or greater than 4. A *GFP Idle Frame* is characterized by PLI and cHEC equal to 0000 hex, and the total frame length is therefore 4 bytes long. The *Payload Area Header* is subdivided into two portions: *Payload Type* and *Extension Headers*. *Payload Type* has 2 octets intended to describe the GFP payload information content. It is subdivided again into 5 portions [3], [49]: *Payload Type Identifier* (PTI), *Payload FCS Indicator* (PFI), *Extension Header Identifier* (EXI), *User Payload Identifier* (UPI) and *Type Header Error Control* (tHEC). The PTI is used to differentiate between the two kinds of client frames: data frames and client management frames. The latter type is used for CSF management. The PFI is used to indicate the presence of the *Optional Payload Frame Check Sequence*. The type of payload information that can be accommodated on GFP-F and GFP-T modes is described by an 8-bit long UPI field. The EXI is used to support client PDU multiplexing in scenarios in which different client traffics share a single GFP link. GFP supports linear and ring topology sharing. The *tHEC* is a 16-bit CRC code used to protect the *Payload Type*. Refer to [3], [48]–[50] for more information about GFP frame control fields.

Section 7 of Recommendation G.7041 [3] standardized the frame-mapping procedure for Ethernet MAC. Figure 2 illustrates this procedure. An Ethernet frame has its *Preamble* and SFD removed, as described in item 7.1.2 of G.7041. The IGP is also removed in the source adaptation process, and the Preample, SFD, and IGP are restored later The remaining fields are accommodated in the GFP-F payload information area. GFP maintains octet alignment. The GFP Payload FCS and the *Extension Header* are optional.

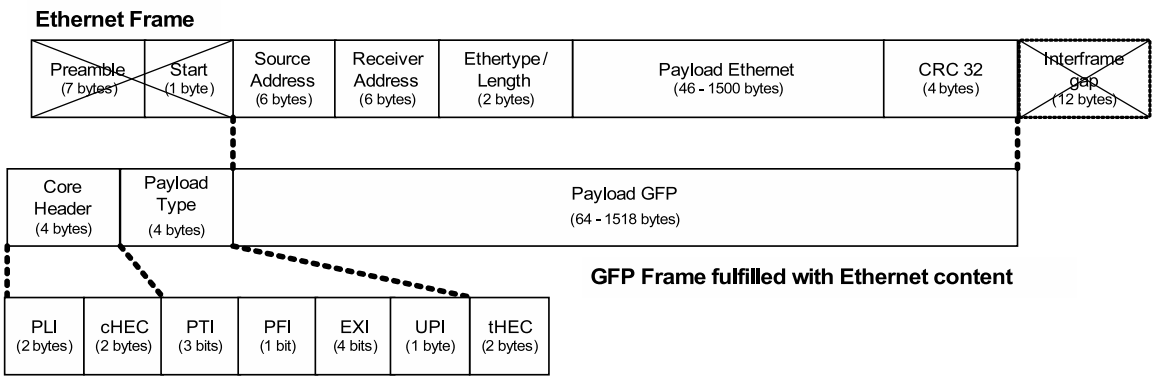

Fig. 2. Encapsulating Ethernet frames using GFP-F.

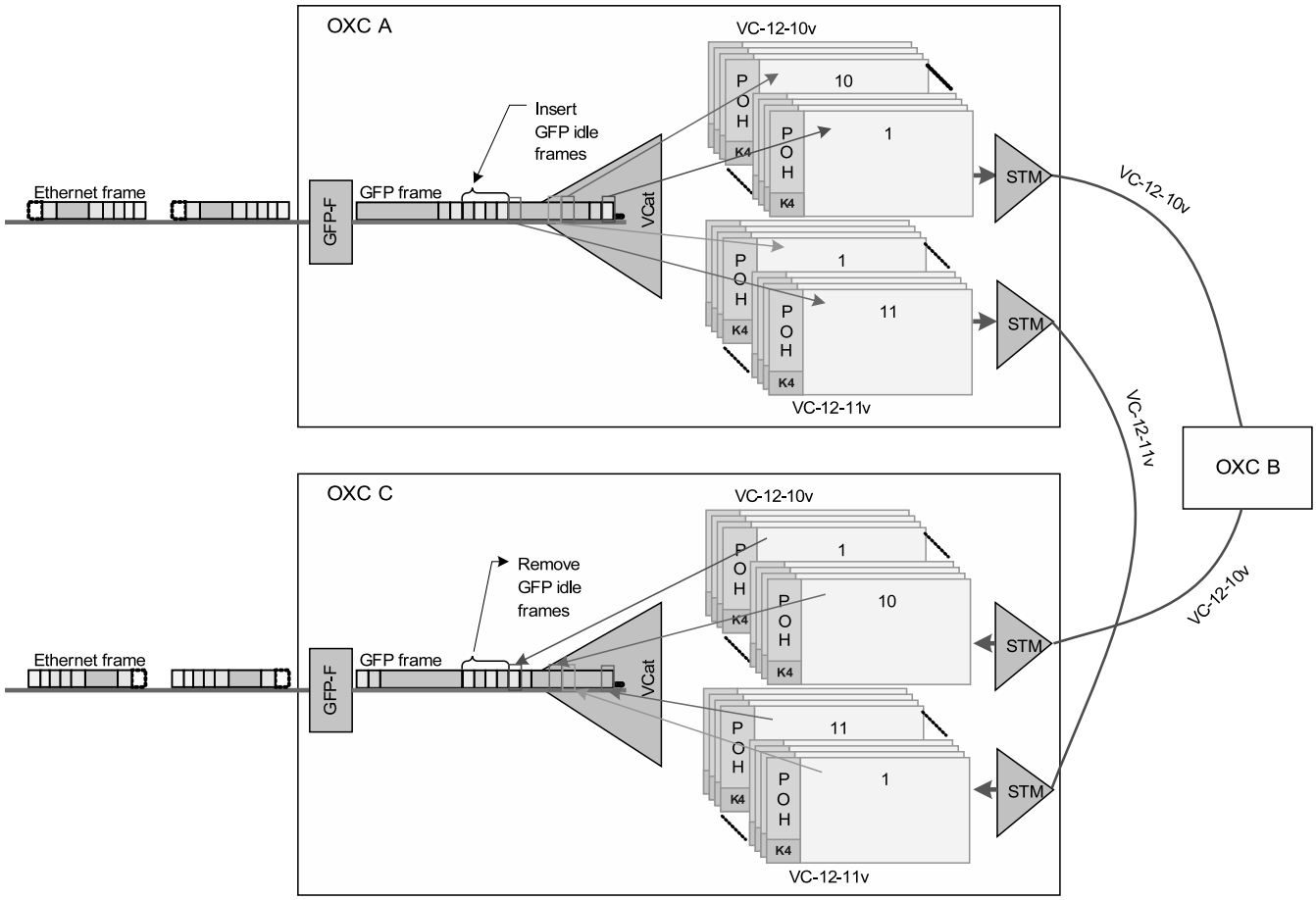

Fig. 3. Functioning of GFP-F and VCat in an EoS network.

GFP-T also allows transparent mapping of Gigabit Ethernet 8B/10B line coding. In GFP-T a fixed number of client octets is mapped to a constant-length GFP frame. Therefore, an Ethernet frame coded with 8B/10B coding will be accommodated into one or more GFP-T frames. GFP-T uses the same GFP-F frame structure, and also provides performance-monitoring capabilities. Gorshe and Wilson [60] and Ellanti et al. [61] provide a detailed description of GFP-T operation.

E. Virtual Concatenation

VCat was originally standardized by ANSI T1.105 [62], ITU-T G.707 [2] and G.783 [63]. It defines an inverted multiplexing scheme, in which a contiguous data rate is broken into individual low- or high-order VCs. Thus, a tributary can be mapped to a combination of VCs that better fits its capacity needs. This combination is called a *Virtual Concatenation Group* (VCG). The nomenclature used is VC-n-Xv, where VC-n is the type of virtual container allowed in the VCG and X is the number of virtually concatenated VCs-n. Other

inverse multiplexing techniques were proposed before VCat, such as [64] *Multi Link Point-to-Point Protocol* (MLPPP) [65] and *Ethernet Link Aggregation* [7]. VCat can be applied to SONET/SDH, OTN or PDH. The latter is standardized in ITU-T G.7043 [66].

VCat arose to overcome waste in the data rate of *contiguous concatenation* when mapping high-rate signals, such as GbE. For example, a GbE MAC frame mapping does not fit into VC-4-4c at 622 Mb/s. The next degree is a VC-4-16c at 2.448 Gb/s. However, this option has an efficiency of 42% [67]. With a VC-4-7v, the data rate efficiency increases to 95%. Therefore, VCat allows transport efficiency to be increased by relaxing CCat granularity [48]. Helvoort [67] determined VCat possibilities and transport efficiencies for a variety of signals.

At the network entrance, VCat performs an inverse multiplexing, accommodating each byte of the high-rate signal into a different VC-n-Xv. In other words, it uses byte-interleaving to put the i^{th} byte of the source content into VC-n-1v, and then the $(i+1)^{th}$ byte is sent out on VC-n-2v, and so on, until a loopback is created and the next byte is sent back on VC-n-1v. Therefore, VCat uses the group transmission capacity of X individual VCs of type *n* to produce a channel with X times more capacity.

Each VC-n has its own individual control overhead and could, therefore, be transported independently over the network. This is another advantage that VCat has over CCat. Each VC-n can be spread out over diverse paths to increase reliability against failures. Also, a cross-connect does not need to know that the data transported in a certain VC-n-1v are related to the data transported in another VC-n-2v, and so on. Therefore, each VC-n-Xv can take a different path over the network, experiencing different delays. The difference among these delays is known as the *differential delay* [68]. In the far-end network equipment, all of these VC-n-Xv are multiplexed back. Therefore, the end equipment must re-establish the byte order from each received VC-n-Xv byte. The de-interleaving process does not introduce significant delays. The most significant delay is the propagation delay of the longest VC-n path.

The maximum *differential delay* standardized for VC-11-Xv, VC-12-Xv and VC-2-Xv, VC-3-Xv and VC-4-Xv *virtual concatenations* is limited to 256 ms. The same value applies to E1-Xv. This value is very big and allows VCat employment in WANs.

VCat's capacity to use disjoint paths increases the probability of new flow admission as well as the network resource usage. In other words, VCat allows the use of disjoint VCs-n to increase client traffic flow admission. As the acceptance grows, the usage increases. Together with LCAS, VCat allows VCs-n to be re-routed to provide network maintenance and/or traffic engineering. Operators can use VCat capabilities to provide on-demand adjustments to client traffic and scheduled data rate patterns. *Service Level Agreements* (SLAs) can be more dynamic, allowing pay-per-use scenarios.

For high-order VCat channels, including VC-3-Xv and VC-4-Xv, the differential delay is measured by examining the *Multi-Frame Indicator* (MFI) that is part of each VCG member's POH. The MFI is located in the H4 byte, and is incremented in each frame for each member of the VCG. According to [70], "*the evaluation of differences in MFI values between members will reflect the differential delay between any two members that are part of a VCG*." For low-order VCat channels, including VC-11-Xv and VC-12-Xv, it is necessary to indicate the VC-n-Xv frame count using bit 2 of the POH Z7/K4 channel. This information is contained in 32 bits. Thus, it is necessary to receive 32 multiframes (with 4 frames each) to fully recover this information, resulting in a frame count cycle of 128 frames (or 16 ms).

Figure 3 illustrates how GFP-F adapts Ethernet frames for transportation in two disjoint paths over an SDH network: one direct path from OXC A to C and one path passing through OXC B. First, GFP-F encapsulates each Ethernet frame in a GFP frame, inserting *GFP Idle Frames* in the absence of Ethernet frames (the spaces between adjacent Ethernet frames). The resultant GFP-F stream (constant bit rate) is byte-interleaved in such a way that the first byte of the GFP stream is put into the first VC-12 of the VC-12-10v. The second byte is put into the second VC-12 of the VC-12-10v, and so on, until byte ten of the GFP stream is put into the tenth VC-12 of the VC-12-10v. The procedure continues interleaving one byte into each VC-12 of VC-12-11v, until a loopback is created, sending the 22nd byte in the first VC-12 of VC-12-10v. Both VCs-12-Xv are accommodated by SDH multiplexing on different STMs, which are transported on disjoint fiber optics to other SDH equipment. At OXC C, both VCs-12-Xv are multiplexed again (after differential delay compensation) to rebuild the original GFP frame stream. Any *GFP Idle Frames* are removed and the Ethernet frames are rebuilt.

F. Link Capacity Adjustment Scheme

The LCAS protocol was standardized in ITU-T G.7042/Y.1305 [4] in November 2001. The latest review was in March 2006. The main goal of LCAS is to adjust link capacity dynamically according to source and/or destination needs. It provides control and management mechanisms to increase or decrease a VCG's capacity in multiples of a VC-n-1v. LCAS automatically increases and decreases the number of VCs-n in a VC-n-Xv. If the physical link of a group member VC-n suffers a failure, LCAS automatically decreases the number of VCs-n in the VC-n-Xv, becoming a VC-n-(X-1)v. As a consequence, the client flow is spread out over the (X-1) VCs-n. When the physical link failure is repaired, LCAS automatically increases the number of VCs-n in the VC-n-(X-1)v, returning to a VC-n-Xv configuration [64]. This procedure reduces client traffic losses, because the other (X-1) VCs-n remain intact in the event of a simple link failure. These group changes do not interrupt transport service. In addition, the core nodes are transparent for LCAS procedures.

Therefore, LCAS acts to limit failure damage in a virtual concatenated VC. According to [11], "*this important LCAS functionality allows a provider to improve significantly the resiliency offered to end users by provisioning diversely routed SONET/SDH paths that belong to the same VCG.*" Thus, if

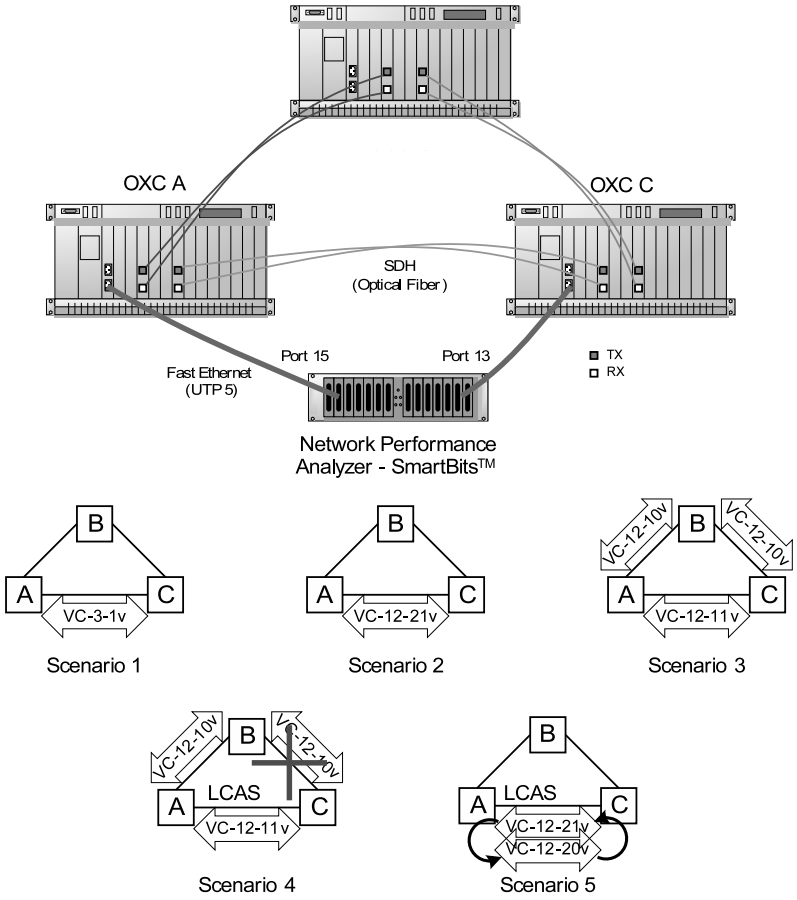

Fig. 4. Network topology and configured scenarios used in laboratory experiments.

diverse routing is used, LCAS could improve the survivability of data traffic without requiring excess data rate allocation for protection.

When LCAS is enabled, link capacity adjustment controls are sent using the VC-n's POH. For VC-3 and VC-4, The H4 byte is used, while for VC-11, VC-12 and VC-2, bit 2 of the Z7/K4 channel is used. These controls Include: the MFI, used to realign the payload of VCG members; the *Sequence Indicator* (SQ), which contains the sequence number of a certain VCG member, i.e., it differentiates the VCs-n inside a VCG; the *Control* (CTRL) field, which allows the source and destination to agree about the VCG members by sending commands to change the number of VCG members in a VC-n-Xv as well as determining the VCG's status; the *Group Identification* (GID), which identifies the CVG and is used by the receiver to determine which VCG a member belongs to; CRC, for error protection in the LCAS controls; the *Member Status* (MST) field, which reports an individual member's status (OK or FAIL) to the transmitter; and *Re-Sequence Acknowledge* (RS-Ack) to inform the transmitter about VCG members that have been received successfully. Other references for LCAS are [4], [11], [46], [59], [64].

3. Previous Work on Ethernet-over-SDH Transport Performance

Bonenfant and Rodriguez-Moral [48] discussed Ethernet and GbE over SDH in 2001. The paper described three possibilities for transporting physical-layer GbE signals, which are 1.25 Gb/s 8B/10B encoded bit streams: a single WDM wavelength, a single STM-16 or STM-64 to multiplex 1 GbE signals statistically, or 7 virtually concatenated VC-4s (VC-4-7v). Reference [48] briefly presented GFP, VCat and LCAS, and argued that the combination of these technologies "*offers an attractive option for carrying data networking protocols over transport networks, and presents an alternative to the use of ATM and MPLS for transport-oriented statistical multiplexing gain*."

In 2002, Scholten et al. [50] provided an introduction to applications for data transport over SONET/SDH, reviewed existing data transport options (as shown in Figure 1), introduced GFP as a new data transport technology and compared GFP transport to popular existing alternatives. The paper argued that "GbE does not fit into STS-12c/VC-4-4c at 622 Mb/s, and wastes data rate if mapped singly into a 2.448 Gb/s (STS-48c/VC-4-16c)." It then provided a discussion about how VCat can be used to solve this problem. Another paper, from Bonenfant and Rodriguez-Moral [59], also discussed GFP in 2002. A comprehensive discussion about mapping options before the arrival of GFP was provided. The authors contend

that "the attractiveness of GFP lies in its combination with the co-developed VCat and LCAS." Also, the paper contends that 100 Mbit/s Fast Ethernet frame traffic can be mapped to a VC-11-64v with 98% bandwidth efficiency, and that 1 GbE frame traffic can be mapped to a VC-4-7v with 95% bandwidth efficiency. Gorshe and Wilson [60] also published a paper about GFP and its role in EoS. Bonenfant and Rodriguez-Moral [48], [59] presented VCat mapping possibilities for ESCON, Fibre Channel, FICON and GbE.

In 2002, Li et al. [51] still proposed a hardware architecture to encapsulate Ethernet frames using VC-12-Xv. The authors proposed a solution to deal with the different path delays experienced by VCG members at the receiver side. The compensation was performed by jumping to different writing addresses in physical memory based on each VCG constituent's MFI. The paper also proposed an approach to receiver queue dimensioning that deals with this delay.

Another 2002 paper that proposed a hardware architecture that uses VCat for EoS was published by Shi et al. [69]. In this work, a proposal to compensate the *differential delay* was presented. Garg and Paul [68] presented a differential delay handler for a SONET frame receiver. The handler is composed of an array of *Random Access Memory* (RAM), which is used to store each received VC-n-Xv group member bit stream. There is also a classifier that uniquely identifies each received VC-n based on its H4 byte or K4 byte, depending on VC type. After classification, a memory controller chooses RAM to store the VCs-n being received. A calculator determines the current *differential delay* based on stored streams, and delay compensation is performed by realigning the VCs from stored frames. According to the authors, "*the amount of storage depends on the maximum differential delay required*." As previously described, ITU-T recommends a maximum of 256 ms for a VC-n-Xv. However, typical values are equivalent to 256 frames or $125\mu s * 256 frames = 32ms$ [68]. This results in a 75 Mbit [68] storage requirement to compensate +/- 16 ms of *differential delay* at OC-48/STM-16 speed. The work also discussed what types of memory could be used to fulfill this high-density memory requirement.

In 2004, Ramamurti et al. [12] highlighted some important issues regarding EoS deployment. The paper discussed the impact of *Inter-Frame Spacing* on Ethernet mapping over SDH. According the authors, IFS can vary from 20 bytes to greater values to adjust the nominal data rates of Ethernet frames to SONET/SDH rates. The authors also warned that "*Ethernet frame loss can occur when the Ethernet source generates traffic at full line rate (100 percent utilization), even when the SONET/SDH bandwidth greatly exceeds the required Ethernet bandwidth*." Finally, the work questioned the importance of performance monitoring on EoS networks.

Barlow [70] discussed Ethernet delay in EoS in a 2004 white paper. The paper focused on the several components that contribute to the total delay in EoS and briefly discussed the measurement techniques necessary to experimentally evaluate performance. The methodology described by Barlow is based on RFC 2544 [71]. We also used this methodology as will be presented in Subsection 5.A.

In 2005, Dahai [72] compared GFP to LAPS Ethernet encapsulation over SDH. Some experiments have been performed on hardware to evaluate the frame loss rate of both protocols. The author's conclusion was that "*frame length is a key factor of network performance in data transmission. It is obvious that GFP has some advantages than LAPS in the demand-based data service network*." In 2005, Gunreben and Gauger [73] proposed dynamic bandwidth allocation in EoS using VCat and LCAS. The idea was to dynamically change the number of VCs in a VCG according to traffic demands. An aggregated traffic model was constructed using the M/Pareto distribution, and three controllers for bandwidth estimation were developed. The paper also discussed traffic scenarios in which dynamic data rate allocation could improve EoS efficiency.

Ge and Yoshimura [74] presented the design and implementation of an EoS chip. The proposed chip structure allows the internal workings of EoS hardware to be understood. The paper also discussed the role of buffers in the rate adaptation problem. A mathematical queuing theory traffic model was used. In our work, we used real equipment rather than an emulator or simulator, as will be discussed in subsection 5. Therefore, we did not have access to the equipment architecture, which complicated any kind of queuing model.

Kuri et al. [75] quantified the savings that VCat provides over CCat. Performance evaluation was done by means of mathematical modeling using combinatorial optimization and computational calculations.

In 2006, Kim et.al. [76] discussed the role of EoS in routing/switching with QoS. This paper also presented a discussion about the evolution of EoS as well as a hardware solution called the *QoS Switch/Router* (QSR). Some details of the hardware were presented. Also in 2006, He et al. [11] discussed three Ethernet transportation technologies: *transporting Ethernet services over a pure switched Ethernet network, over an IP /MPLS network and over the SDH-based Multiservice Transporting Platform (MSTP)*. More interestingly, the final section of the paper provided a performance evaluation of these Metro Ethernet transportation services in terms of encapsulation efficiency, end-to-end delay and fault protection. The presented efficiency results will be compared with the ones discussed in this paper in Subsection 5.C.4.

In another 2006 paper, Bernstein et al. [64] summarized the capabilities and limitations of the application of VCat/LCAS not only in SDH, but also in PDH and OTN. The authors argued that the total delay of an aggregated signal will be equal to the delay of the component signal that travels along the longest path. The paper also presented the maximum differential delay and the LCAS notification time of various VCat signals, according to given standards. Tzeng and Chiu [77] proposed a hardware architecture to transport 4 GbE and 20 Fast Ethernet signals over an OC-48 SONET connection. The paper discussed several tradeoffs in VCat/LCAS hardware design. It also provided a solution to minimize memory usage when solving the *differential delay* problem.

Finally, in 2007, Wentao et al. [78] discussed two schemes for Ethernet over E1 (PDH). The paper evaluated the throughputs and delay performances of these schemes. Analytical results were compared with experimental test results obtained

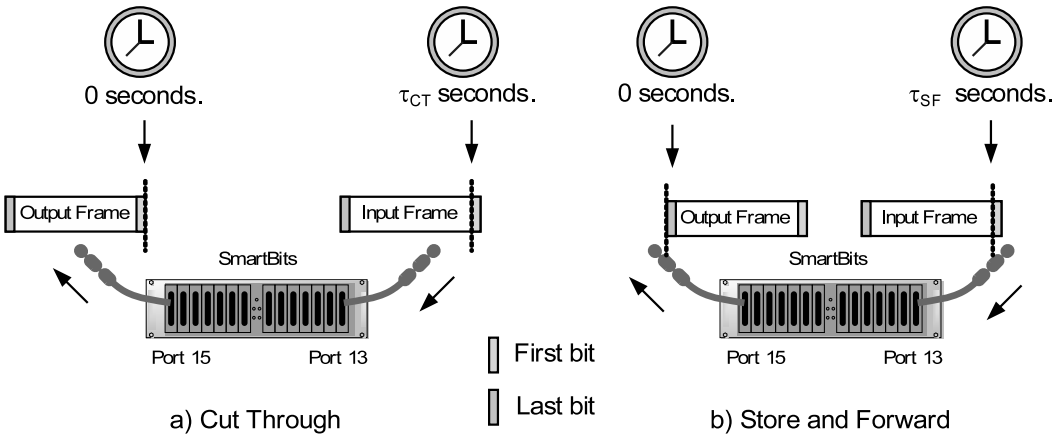

Fig. 5. Methods of measuring delay.

from a *Field Programmable Gate Array* (FPGA) implementation.

4. Analytical Treatment of Throughput, Efficiency and Delay in EoS

GFP frames are accommodated in VCs-n-Xv, and therefore the expressions derived here are for GFP-F mode only. To our knowledge, we do not found in the literature a set of equations like this. It is assumed that no Ethernet frames are lost in the encapsulation/mapping procedure, and the Ethernet traffic is assumed to be controlled to achieve this assumption of lossless encapsulation. The SDH network is assumed to be error-free.

The GFP frames per second that can be mapped in a VC-n-Xv is given by:

$$\hat{FR_{GFP}} = \frac{MBR_{VC-n-Xv} * 10^6 bps}{8bits * (Payload_{GFP} + 8bytes)} \quad (1)$$

Where $MBR_{VC-n-Xv}$ is the nominal Megabit rate of the VC-n-Xv used in VCat, and $Payload_{GFP}$ is the length, in bytes, of the content encapsulated in a GFP frame payload. As shown in Figure 2, $Payload_{GFP}$ is the Ethernet payload plus an additional 18 bytes. Because each Ethernet frame that passes EoS hardware is mapped to only one GFP frame, there is a one-to-one relation between the number of transmitted Ethernet and GFP frames. Therefore, the variable $\hat{FR_{GFP}}$ is equal to $\hat{PFR}_{Eth}$, which is defined as the passed Ethernet frame rate. It is also useful to derive the maximum Ethernet frame rate that can be received in the link that delivers the frames to the EoS hardware:

$$\hat{MFR}_{Eth} = \frac{Capacity_{Eth} * 10^6 bps}{8bits * (Payload_{GFP} + 20bytes)} \quad (2)$$

Where $Capacity_{Eth}$ is the Megabit rate of the Ethernet line to the EoS hardware.

From equation (1), it is possible to derive the number of GFP frames transmitted in t seconds $\hat{XmtFrames}_{GFP} = \hat{FR_{GFP}} * t$.

The number of GFP frames received in t seconds, $\hat{RcvFrames}_{GFP}$, is equal to the number of transmitted GFP frames. Therefore, $\hat{RcvFrames}_{GFP} = \hat{XmtFrames}_{GFP}$. An equation can also be derived for the number of GFP payload bytes received in t seconds $\hat{RcvPayloadBytes}_{GFP} = \hat{RcvFrames}_{GFP} * Payload_{GFP}$.

Still using (1), the Megabit rate of Ethernet can be obtained from:

$$\hat{MBR}_{Eth} = \frac{8bits * \hat{FR_{GFP}} * (Payload_{GFP} + 20bytes)}{10^6 bps} \quad (3)$$

It is also possible to calculate the percentage of $\hat{MBR}_{Eth}$ that can be accommodated by the SDH network. It is given by $\hat{\%Passed}$ and calculated by dividing $\hat{MBR}_{Eth}$ by $Capacity_{Eth}$.

From Figure 2, it is also possible to determine the effective Megabit rate available for Ethernet clients ($\hat{MBR}_{Client}$), which is defined as:

$$\hat{MBR}_{Client} = \frac{\hat{FR_{GFP}} * [Payload_{GFP} - 18bytes] * 8bits}{10^6} \quad (4)$$

Based on the same figure, $\hat{MBR}_{PayloadGFP}$ can be calculated from $\hat{FR_{GFP}} * Payload_{GFP} * 8ns$. The Megabit rate of GFP frames, $\hat{MBR}_{GFP}$, is given by $\hat{MBR}_{GFP} = \hat{FR_{GFP}} * [Payload_{GFP} + 8] * 8ns$. Note that this expression will produce the same value as $MBR_{VC-n-Xv}$, because both rates are considered to be the same. The Megabit rate of Ethernet frame headers ($\hat{MBR}_{EthHeader}$) can be defined as $\hat{MBR}_{EthHeader} = \hat{MBR}_{PayloadGFP} - \hat{MBR}_{Client}$. It is also possible to determine $MBR_{GFPHeader}$, which is the Megabit rate expended on GFP headers and is calculated by $\hat{MBR}_{GFPHeader} = \hat{MBR}_{GFP} - \hat{MBR}_{PayloadGFP}$.

Two variables describing efficiency can be used: the GFP encapsulation efficiency, defined as:

$$\hat{\eta 1_{GFP}} = \frac{\hat{RcvPayloadBytes}_{GFP}}{\hat{RcvFrames}_{GFP} * (Payload_{GFP} + 8bytes)}, \quad (5)$$

and the efficiency of EoS, defined as:

$$\hat{\eta 1_{EoS}} = \frac{(\hat{MFR}_{Eth} * \hat{\%Passed}) * (Payload_{GFP} - 18) * 20}{\hat{RcvFrames}_{GFP} * (Payload_{GFP} + 8)}. \quad (6)$$

The most important components of the delay in Ethernet over SDH networks using GFP, VCat and LCAS Are the propagation, emission and differential delays. The first emission delay that can be considered is the Ethernet frame emission delay:

$$\hat{\tau_{Eth}} = \frac{(Payload_{GFP} + 20bytes) * 8bits}{Capacity_{Eth} * 10^6 bps} \quad (7)$$

Note that this delay also occurs at any SDH destination equipment, as every Ethernet frame must be emitted to the destination Ethernet switch.

A second emission delay to consider is the GFP frame emission delay, which appears when a GFP frame is transmitted as a VC-n-Xv. It is given by:

$$\hat{\tau_{GFP}} = \frac{(Payload_{GFP} + 8bytes) * 8bits}{MBR_{VC-n-Xv} * 10^6 bps} \quad (8)$$

Propagation delay depends on the link length and on the velocity of the light in the fiber optic medium. The differential delay depends on the path differences experienced by each VC-n-Xv. The solution adopted to deal with this delay may also add implementation-dependent delays.

5. Experimental Measurement and Performance Evaluation

This section presents results from an experimental performance evaluation of EoS scenarios as well as a comparison with the expressions presented previously. Five scenarios will be examined, and the resulting throughputs, efficiencies and delays will be presented and discussed.

A. Experimental Network Configuration and Measurement Set-up

Figure 4 shows the considered network topology. It is composed of three realistic cross-connects with support for NG-SDH and a network performance analyzer. In this section, the experimental results obtained using a SmartBits^{TM} performance tester will be presented and discussed.

The SmartBits equipment facilitates performance evaluation of Ethernet-inter-connected devices. The equipment uses a performance benchmarking methodology specified in RFC 2544 [71]. In this methodology, the transmitter sends a certain number of frames over a pre-defined time interval. If some frames are lost, the equipment discards the measurement and tries again with a minimal number of frames. If no frames are lost with this minimal quantity, the equipment tries to increase the number of transmitted frames, until it reaches a maximum number of frames that can be transmitted without loss. Therefore, measured results were obtained only if no Ethernet frames were lost.

In order to compare the overhead of different scenarios, we used the same time duration for all experiments. This explains why we do not use experiment duration times that are integer multiples of Ethernet frame emission times. The objective was to compare absolute results of 20 second experiments. However, this approach led to some discrepancies due to frame fragments.

From field experience, and because SDH networks are deterministic and very stable, we determined that 20 seconds would be sufficient time to obtain satisfactory results and validate analytical expressions. During experimentation, the laboratory temperature and humidity were kept constant, the same synchronization reference was used and the equipment energy source was stabilized, thereby eliminating various important sources of variation and maintaining a consistent test scenario during all measurements. In addition, the number of frames transmitted in 20 seconds was large enough to ignore transitory behavior.

In the first scenario, a VC-3-1v was directly established between OXCs A and C of Figure 4. In the second scenario, a VC-12-21v, which is 21 virtually concatenated VC-12s, was directly established between OXCs A and C. In scenario three, a VC-12-21v was established using two different paths. A VC-12-11v was directly established between OXCs A and C, while a VC-12-10v was established from OXC A to B, and then from OXC B to C. Notice that the third scenario is almost identical to the second one, except for the employed path. Scenarios 4 and 5 used LCAS. In scenario 4, link B-C was torn down and LCAS was automatically used. In scenario 5, LCAS was used to decrease/increase a VC-12-21v by one VC-12.

The SmartBits equipment was used to generate Ethernet traffic, to adjust frame size and rate, and to measure results. The experiments used two ports of the equipment (see Figure 4), one to transmit traffic (port 15) and other to receive traffic (port 13) and measure results. $SmartApplications^{TM}$ version v2.32 was used, which transmits fixed-length frames at 100 Mbit/s. Data were collected for frame sizes of 64, 256, 512, 1024 and 1518. For each frame size, the sequence of frames was encapsulated into GFP without loss, using the available bandwidth in this VC.

As can be seen in [11], the latency tests were done after throughput tests, at a rate below the minimum rate that caused frame loss. This prevents the loss of timestamp-tagged frames in latency tests.

B. Experimental Performance Metrics

This section describes the several metrics that SmartBits equipment uses to experimentally determine Ethernet performance.

The Ethernet frame rate submitted to achieve 100 Mbit/s at the beginning of the experiment is given by MFR_{Eth}. This measure includes 12 bytes of interframe gaps. Note that the Ethernet frame rate required to achieve 100 Mbit/s can be obtained from the measured data by using $MFR_{Eth} * (Payload_{GFP} + 20bytes) * 8bits$.

FR_{GFP} is the number of GFP frames transmitted in one second to achieve a certain VC-n-Xv rate.

$\%Passed$ gives the percentage of MFR_{Eth} that passed to the SDH network without loss, and is equal to FR_{GFP} divided by MFR_{Eth}.

The measurements $XmtFrames_{GFP}$, $RcvFrames_{GFP}$, $RcvPayloadBytes_{GFP}$ and $RcvPayloadBytes_{GFP}$ are counters. $XmtFrames_{GFP}$ is the total number of GFP frames transmitted within 20 seconds, which was the time

interval chosen for the test. $RcvFrames_{GFP}$ is the total number of GFP frames received on port 13 of the SmartBits equipment.

If the beginning of a GFP frame arrived at the SmartBits after exactly 20 seconds, it was counted as an entire received frame. However, only the received bytes were counted in the variable $RcvPayloadBytes_{GFP}$. This leads to some discrepancy among the measured variables, as $RcvFrames_{GFP}$ is an integer number. $RcvPayloadBytes_{GFP}$ is the total amount of bytes received in GFP payloads. Therefore, $RcvPayloadBytes_{GFP} = RcvFrames_{GFP} * Payload_{GFP}$. The FR_{GFP} variable can be related to $RcvPayloadBytes_{GFP}$ by $FR_{GFP} = RcvFrames_{GFP}$ divided by t=20 seconds.

The delay measure τ_{CT} is the difference between the time that the end of the first bit of the input frame reaches the input port (port 13 of SmartBits) and the time that the start of the first bit of the output frame is seen on the output port (port 15). The measure τ_{SF} is the difference between the time that the first bit of the input frame reaches the input port (port 13) and the time that the last bit of the output frame is seen on the output port (port 15). Figure 5 illustrates these measurement methods used by the $SmartApplications^{TM}$ v2.32 software. The difference between τ_{SF} and τ_{CT} is the Ethernet frame emission delay $\Delta\tau = \tau_{CT} - \tau_{SF}$.

C. Throughput and Efficiency Results

1) First Scenario: Ethernet/GFP/VC-3-1v: In this scenario, a VC-3-1v, which is a virtually concatenated VC-3, was established directly between OXCs A and C of Figure 4. A VC-3-1v has 48.384 Mbit/s available for payload, as C-3 has 9 lines versus 84 columns of payload capacity, which are transmitted every 125 μ seconds. Table I shows that as the frame size increased, FR_{Eth} and $XmtFrames_{GFP}$ decreased, while $RcvPayloadBytes_{GFP}$ increased. In other words, as the length of the GFP payload increased ($Payload_{GFP}$), more bytes were received and the Ethernet frame (+gap) rate decreased, along with the number of transmitted GFP frames. It can also be seen that the number of transmitted GFP frames ($XmtFrames_{GFP}$) was equal to the number of received frames ($RcvFrames_{\ GFP}$), confirming that no Ethernet frames were lost in this experiment.

In Table III, the experimental results were used as input to the analytical expressions to allow comparisons between calculated and measured quantities. We use a tilde over semi-analytical variables. From Table I, $\tilde{FR_{GFP}}$ was 83893 GFP frames per second when $Payload_{GFP}$ was equal to 64 bytes. The Ethernet header occupies 18 bytes of this 64 bytes. Thus, $\tilde{MBR_{EthHeader}}$ was equal to 12.080592 Mbit/s. The GFP header occupies another 8 bytes of this 64, wasting another 5.37 Mbit/s ($\tilde{MBR_{GFPHeader}}$). When $Payload_{GFP}$ is equal to 1518 bytes, $\tilde{FR_{GFP}}$ is reduced to 3968 GFP frames. The Ethernet header occupies 18 bytes of this 1518 bytes, wasting 0.843696 Mbit/s ($\tilde{MBR_{EthHeader}}$). The GFP header occupies another 8 bytes of this 1518, wasting 0.25 Mbit/s ($\tilde{MBR_{GFPHeader}}$). In summary, the bit rate available for clients ($\tilde{MBR_{Client}}$) increases with $Payload_{GFP}$, confirming that a larger payload area increases the available bit rate for clients. The VC-3-1v capacity is approximately equal to the Megabit rate of GFP frames ($\tilde{MBR_{GFP}}$).

As expected, the GFP encapsulation efficiency $\tilde{\eta 1_{GFP}}$, as defined by equation (5), increased from 88.89% to 99.48% when $Payload_{GFP}$ was increased from 64 bytes to 1518 bytes, for an improvement of 11.91%. The fraction of resources devoted to overhead decreases as frame size increases, thus increasing the resources available for payload and improving efficiency. The EoS encapsulation efficiency $\tilde{\eta 1_{EoS}}$, as defined by equation (6), increased from 63.89% to 98.29%. As expected, overall EoS encapsulation efficiency is less than that of standalone GFP technology, as GFP has less overhead.

Table II shows the analytical calculations for Scenario 1. The measured FR_{GFP} for $Payload_{GFP}$ equal to 64 bytes was 83893 frames/second, while the calculated result, $\hat{FR_{GFP}}$, was 84000 frames/second, 0.1275% higher than the measured value. For $Payload_{GFP}$ equal to 1518 bytes, the measured FR_{GFP} was 3968 frames/second, while the calculated value, $\hat{FR_{GFP}}$, was 3963.3 frames/ second, 0.1183% smaller than the measured value.

All of the values in both tables were compared and the error in the analytical expressions was limited to 0.12802%. In summary, when Table II is compared with Table I, it is seen that the derived expressions satisfactorily approximate the measured results. Interestingly, the difference between the analytical expressions and the measured data was reduced as $Payload_{GFP}$ was increased.

2) Second Scenario: Ethernet/GFP/VC-12-21v: In the second scenario, a VC-12-21v, which is 21 virtually concatenated VC-12s, was established directly between OXCs A and C of Figure 4. A VC-12 has 2.176 Mbit/s of payload, as a C-12 has 34 bytes of payload capacity transmitted every 125 μseconds. To understand why this VCat configuration was chosen, it is necessary to remember that a *Tributary Unit Group* 3 (TUG-3) can be formed by one VC-3 or 21 VCs-12. Therefore, the two signals are similar from the TUG-3's point of view, but a VC-12-21v has 21 x 2.176 Mbit/s, or 45.696 Mbit/s, while a VC-3 has 48.384 Mbit/s.

Table IV shows that FR_{Eth} and $XmtFrames_{GFP}$ decreased as $Payload_{GFP}$ increased, as in Scenario 1. The number of transmitted GFP frames ($XmtFrames_{\ GFP}$) was equal to the number of received frames ($RcvFrames_{GFP}$). In Table VI the experimental results were used as input to the analytical expressions. The Ethernet overhead for all $Payload_{GFP}$ was larger than that of GFP-F. Again, the bit rate available for clients ($\tilde{MBR_{Client}}$) increased with $Payload_{GFP}$. The Megabit rate of GFP frames ($\tilde{MBR_{GFP}}$) was slightly higher than the VC-12-21v capacity, as the measurement included frames that were not entirely received during the 20 second time interval.

The GFP encapsulation efficiency $\tilde{\eta 1_{GFP}}$ increased from 88.89% to 99.48% when $Payload_{GFP}$ increased from 64 bytes to 1518 bytes. The EoS encapsulation efficiency $\tilde{\eta 1_{EoS}}$ increased from 63.89% to 98.29%. This occurred because as the frame gets larger, the overhead has less of an effect on the EoS efficiency. Table V shows the analytical results for Scenario 2. All of the values in both tables were compared

and the difference between the computed and measured results was limited to 0.118544%.

3) Third Scenario: Ethernet/GFP/(VC-12-10v+VC-12-11v): In this scenario, a VC-12-21v was established using two different paths. A VC-12-11v was established directly between OXCs A and C of Figure 4, while a VC-12-10v was established from OXC A to B, and then from OXC B to C. Both virtual concatenated VCs have a capacity of 45.696 Mbit/s. Note that this scenario produced results almost identical to the previous scenario. The main difference was the path that VCat used. However, in contrast to what one might think, the results are identical to those presented in Section 532. That is, there was no measured difference in the throughputs and efficiencies of scenarios 2 and 3, and the VCat mechanism does not affect these metrics in the considered scenarios.

4) Discussion: Scenarios 1, 2 and 3: Figure 6 compares the measured MFR_{Eth} with the analytical $\hat{MFR}_{Eth}$ for the three scenarios. The number of Ethernet frames (+gaps) per second submitted by SmartBits is equal in all scenarios to allow for comparison among them. Observe that the Ethernet frame rate if larger for smaller GFP frames, because every Ethernet frame is accommodated in exactly one GFP frame.

FR_{GFP} was greater in Scenario 1 than in Scenarios 2 and 3 (see Figure 7). This is because a VC-3-v has 2.688 Mbit/s more useful bandwidth than a VC-12-21v (or a VC-12-10v and a VC-12-11v). The difference between GFP frame rates among the scenarios is larger for smaller frames, because more GFP frames were generated when a smaller $Payload_{GFP}$ was used. The $\hat{FR_{GFP}}$ values computed from Equation (1) are quite close to the measured values for all scenarios.

Figure 8 compares the measured percentages of Ethernet traffic passed to SDH without loss. Notice that %Passed depends on the Megabit rate of complete Ethernet frames. Thus, it was reduced when the Ethernet frame size was increased, as there are proportionally fewer header bytes in large frames. This explains why the curve on Figure 8 becomes flat. The analytical $\hat{\%Passed}$ values are quite close to the measured %Passed values.

The 2.688 Mbit/s rate difference between VC-3-1v and VC-12-21v is equivalent to 5.88235% of the VC-12-21v bandwidth. If we increase the obtained $\%Passed$ values in Scenarios 2 and 3 by this amount, they are approximately equal to the $\%Passed$ in Scenario 1. For example, consider the $\%Passed$ for a GFP payload of 64 bytes. In Scenario 1, the $\%Passed$ was equal to 56.38%, while in Scenarios 2 and 3 it was equal to 53.33%. $53.33\% * (1 + 0.0588235) = 56.46\%$, which approximates Scenario 1. This shows that there is proportional behavior in the curve of $\%Passed$ versus $Payload_{GFP}$ for different VCat configurations.

Figure 9 shows the number of GFP frames transmitted in 20 seconds. Notice that $XmtFrames_{GFP}$ and $RcvFrames_{GFP}$ are equal in each scenario, as FR_{GFP} was adjusted to prevent the loss of Ethernet frames. The results of Scenario 1 were a little bit larger than those of Scenarios 2 and 3, again because of the 2.688 Mbit/s rate difference between VC-3-1v and VC-12-21v. Both variables decreased as $Payload_{GFP}$ increased, as explained before. The $\hat{XmtFrames_{GFP}}$ values closely follow the measured number of transmitted GFP frames.

Figure 10 compares $\tilde{MBR}_{Client}$ and $\tilde{MBR}_{Eth}$, which were semi-analytically calculated from the measured data, with $\hat{MBR}_{Client}$ and $\hat{MBR}_{Eth}$, calculated directly from analytic expressions. The throughput available for Ethernet clients ($\tilde{MBR}_{Client}$) increased as the GFP frame increased (as did the payload), because the header remained the same size. The difference in $\tilde{MBR}_{Client}$ and $\tilde{MBR}_{Eth}$ for Scenarios 1 and 2/3 is caused by the difference in the rates of VC-3-1v and VC-12-21v. This figure also allows us to see that $\tilde{MBR}_{Client}$ gets closer to $\tilde{MBR}_{Eth}$ as the EoS efficiency increases, as more bytes are available to the client. The worst case $\tilde{MBR}_{Client}$ was obtained when $Payload_{GFP}$ was 64 bytes long. Therefore, larger frames provide better client rates in these scenarios.

Figure 11 compares $\tilde{MBR}_{PayloadGFP}$ and $\tilde{MBR}_{GFP}$ with $\hat{MBR}_{PayloadGFP}$ and $\hat{MBR}_{GFP}$. The $\tilde{MBR}_{GFP}$ remains nearly constant for all GFP payload lengths. This is because the GFP filled out all of the available VC-n-Xv capacity with reduced Ethernet frames. Note that some calculated $\tilde{MBR}_{GFP}$ values are higher than the available VC-n-Xv capacities, as there were some situations in which incomplete frames were received and counted as complete frames.

Figure 12 compares the Mbit/s wasted in Ethernet and GFP headers. Obviously, the wastes were reduced when SmartBits increased the Ethernet frame lengths. It is important to note that Ethernet overhead wasted 44.45% more bit rate than the GFP overhead in the employed configuration.

Figure 13 compares the GFP and EoS efficiencies calculated by Equations (5) and (6). Interestingly, all of the scenarios produced the same $\eta 1_{GFP}$ and $\eta 1_{EoS}$ at a given $Payload_{GFP}$. This proves that the GFP encapsulation procedure is independent of the VC-n-Xv scenario configured using VCat. The use of different paths for the VC-12-10v and VC-12-11v in Scenario 3 did not affect the efficiency. However, in terms of availability, Scenario 3 offers a configuration that is more resilient to possible path faults. In the event of a path fault, the LCAS protocol must be used. Subsection 535 investigates LCAS usage in this network topology.

Finally, Figure 13 shows a curve of the encapsulation efficiency reproduced from [11]. The encapsulation efficiency is defined as the "*percentage of the link bandwidth used by the payload when transmitting Ethernet traffic*" at 100 Mbit/s. Although this definition is different from the one adopted here, it is possible to see that our curves have a similar shape as that of He et al.

5) Fourth Scenario: Ethernet/GFP/(VC-12-10v+VC-12-11v) using LCAS: In this scenario, LCAS was used to send management information from a VC-n-Xv source to its destination to inform that a link was torn down. When this occurs, the VC-n-Xv capacity is reduced according to the failed virtual concatenated VCs bandwidth. If LCAS is not being used, then all VCs-n-Xv are lost. The configuration of Scenario 3 was used to verify the benefits of LCAS. First, the link between equipment B and C was removed (second column in Table VII). Thus, only the VC-12-11v remained. The number of GFP frames per second passed to complete the VC-12-11v without loss was significantly reduced, by

52.30096%. Notice that the reduction in rate from VC-12-21v to VC-12-11v is equal to 52.38095%. The other variables were similarly affected. The efficiencies defined in Equations (5) and (6) remained the same for three columns. When the link was recovered, the VC-12-10v returned (column three), and the metrics returned to their exact values before the failure. This demonstrates the advantages of LCAS in availability and failure recovery. LCAS offers VC protection when different paths are used to transmit virtual concatenated VCs.

6) Fifth Scenario: Ethernet/GFP/VC-12-Xv using LCAS: In this experiment, we investigated the capacity of LCAS to dynamically decrease and increase virtual concatenated VCs inside a VC-n-Xv. The measurements were done at three moments: before a VC-12 was decreased (VC-12-21v), after it was decreased (to a VC-12-20v) and when LCAS returned the lost VC-12 (VC-12-21v). The VC-12-21v was passed through link A-C as in Scenario 2. Table VII shows the obtained results. $\hat{FR_{GFP}}$ was reduced by 5.00717%. $\hat{MBR}_{GFP}$ was reduced by 2.17984 Mbit/s. Notice that the reduction in rate from VC-12-21v to VC-12-20v is equal to 5%. Again, the other variables were similarly affected. These changes were set up by means of a *Network Management System* (NMS), which configured LCAS to make bandwidth adjustments. It is not necessary to stop service to adjust bandwidth. We confirmed the quotation from [64]: "*VCAT/LCAS itself provides a graceful degradation (reduction of bandwidth) in response to VCat group component failures*."

D. Delay Results

For the delay experiments, SmartBits filled out 30 Mbit/s of the 100 Mbit/s link capacity. The submitted Ethernet frames (+gaps) per second for all scenarios is shown in Table IX. Again, it is possible to confirm the submitted Ethernet traffic by considering $Payload_{GFP}$ to be equal to 64 bytes, as $30Mbit/s = 44643 * (64 + 20bytes) * 8bits = 30000096bps$.

1) First Scenario: Ethernet/GFP/VC-3-1v: Table X summarizes the results for Scenario 1. As expected, the mean total delay increased with the length of $Payload_{GFP}$. The difference between the cut-through and store-and-forward ($\Delta\tau$) measured port-pair latencies is identical for both bit rates. In fact, it was seen that this value is equal to the emission delay of a $Payload_{GFP}$ at 100 Mbit/s. It can be calculated from $\tau_{PayloadGFP} = Payload_{GFP} * 80ns$. For example, consider a GFP payload of 512 bytes. In this case, $\tau_{PayloadGFP} = 512 * 80ns = 40.96\mu s$. This expression follows the results shown in Table X.

Figure 14 compares τ_{CT} and τ_{SF}. It can be seen that the measured cut-through delay is greater than the store-and-forward delay. The figure also presents a curve obtained from He et al. [11]. The authors used a similar methodology to measure the average end-to-end delay in an Ethernet over GFP over VC-12-46v configuration. However, this measurement was taken with a submitted rate of 90% of a Fast Ethernet link. Although this result was obtained with a markedly different configuration and equipment, it is possible to see the same linearly increasing pattern obtained in our results (refer to $\tau_{VC-12-46v}$). A VC-12-46v has a rate of 100.096 Mbit/s.

2) Second Scenario: Ethernet/GFP/VC-12-21v: The port-pair latency for the second scenario is shown in Table XI. The values were considerably larger than those of Scenario 1, basically because VC-12-nv was chosen. For example, consider the smallest delay, which increased from 136.9 μs to 521.3 μs. These values are still very small for the vast majority of network applications. Interestingly, $\Delta\tau$ was identical to that of Scenario 2. Also, an inversion occurred in the measured τ_{CR} and τ_{SF} when $Payload_{GFP}$ was equal to 256 bytes. We were unable to determine the reason for this behavior. Figure 15 compares τ_{CT} and τ_{SF}.

3) Third Scenario: Ethernet/GFP/(VC-12-10v+VC-12-11v): The results for the last scenario are shown in Table XII. They are similar to those of Scenario 2, but slightly larger. VC-12-Xv was used in this situation, as in the previous scenario. $\Delta\tau$ was again identical to those of Scenarios 1 and 2. The measured τ_{CT} and τ_{SF} at 30 Mbit/s remained higher when $Payload_{GFP}$ was smaller than 256 bytes. Above this payload size, both rate configurations produced nearly the same port-pair latencies.

6. Final Remarks

This tutorial presented the main EoS technologies and describing their central features. Previous works concerning EoS performance evaluation were discussed, providing a comprehensive overview of the essential drawbacks. We presented a set of analytic expressions for EoS throughput, efficiency and delay. We also presented a detailed overview of configurations and procedures for measurements, providing a methodology for measurement and performance evaluation of EoS networks. Finally, we discussed the results measured at Telefonica S.A. testbed and compared them to theoretical expressions. It is important to notice that obtained results guided Telefonica S.A. in implementing EoS networks in its real operation network.

When comparing theoretical throughput and efficiency results with measured values, the errors were limited to 0.13%, validating the presented analytical formulations. We observed that the throughputs and efficiencies of Scenarios 2 and 3 were identical, even though different paths were used for the virtually concatenated VC-12s. This demonstrates that despite the use of different paths, SDH maintains throughput and efficiency. Also, as expected, the throughput available for Ethernet clients increased as the Ethernet frame length increased, as the Ethernet and GFP frame overheads were reduced. Therefore, network operators should increase the Ethernet frame length as much as possible to improve throughput and efficiency. The measured EoS throughput for a VC-3-1v could increase from 63.89% to 98.3% if the Ethernet frames (+gaps) were increased from 84 bytes to 1538 bytes, representing an improvement of 53.85%.

The overhead wastes for Ethernet and GFP were analyzed, and it was shown that Ethernet wastes 44.45% more bandwidth than GFP, although there were significant differences between the roles of Ethernet and GFP on the network. This also demonstrates the efficiency wastes that must be tolerated when interconnecting two technologies not originally designed to work together.

Two latency performance measurements were analyzed: cut-through and store-and-forward. We noticed that the difference between them was identical for all scenarios and increases with the GFP Payload length. In fact, this difference is equal to the emission delay of a GFP Payload at 100 Mbit/s, and it is caused by the measurement procedure. The Cut-through delay values of Scenario 2 were considerably larger than those of Scenario 1, even though no different paths were used in VCat. We suppose that the equipment used different treatments for VC-12-nv and VC-3-1v. The measured latency of Scenario 3 was a slightly larger than that of Scenario 2, because two different paths were used on VCat. Generally speaking, the lossless experiments demonstrated that the measured delay is "well-behaved", regardless of the mapping hardware.

We also used LCAS to send management information from a VC-n-Xv source to its destination, informing the destination where a fiber link was torn down. When this operation occurred, the number of GFP frames per second passed to complete the VC-12-11v without loss was significantly reduced, by 52.30096%. The efficiency remained the same. When the link was recovered, the performance metrics returned to the exact values they had before the failure, demonstrating the graceful operation of LCAS. Also, we investigated the capacity of LCAS to dynamically decrease and increase virtual concatenated VCs in a VCG. The paper qualitatively demonstrated the advantages of LCAS in failure recovery and bandwidth adjustment.

Future works include application of EoS technologies on Carrier Ethernet context as well as convergence of EoS with MPLS, GMPLS, GELS and WDM. Another point is how EoS technologies can help to cope with the exponential growth of video traffic. Also, to investigate how EoS solutions are used in the real network, and how does it work.

7. Acknowledgments

We would like to thank Telefonica S.A. and INATEL. Also, we would like to thank Bruno de Oliveira Monteiro by the preliminary data analysis, help on initial discussions and formulations.

Appendix

ANSI - American National Standards Institute
ATM - Asynchronous Transfer Mode
AU - Administrative Unit
AUG - Administrative Unit Group
CCat - Contiguous Concatenation
CESoE - Circuit Emulation Services over Ethernet
cHEC - Core Header Error Control
CRC - Cyclic Redundancy Check
CRTL - Control
CSMA/CD - Carrier Sense Multiple Access with Collision Detection
DIX - DEC-Intel-Xerox
CSF - Client Signal Fail
CT - Cut-through Delay
EoS - Ethernet-over-SDH
EPL - Ethernet Private Line
EPON - Ethernet Passive Optical Network
ESCON - Enterprise Systems Connection
EVC - Ethernet Virtual Connection
EVPL - Ethernet Virtual Private Line
EVPLAN - Ethernet Virtual Private LAN
EXI - Extension Header Identifier
FCS - Frame Check Sequence
FICON - Fiber Connectivity
FPGA - Field Programmable Gate Array
GbE - Gigabit Ethernet
GELS - GMPLS Controlled Ethernet Label Switching
GFP - Generic Framing Procedure
GFP-F - GFP-Framed
GFP-T - GFP-Transparent
GID - Group Identification
HDLC - High-Level Data Link Control
HEC - Header Error Check
IEEE - Institute of Electrical and Electronics Engineers
IETF - Internet Engineering Task Force
IFS - Inter-Frame Spacing
IP - Internet Protocol
IPG - Inter-Packet Gap
ITU-T - International Telecommunication Union - Telecommunication Standardization Sector
LAN - Local Area Network
LAPS - Link Access Procedure for SDH
LCAS - Link Capacity Adjusting Scheme
LOF - Loss of Frame
MAC - Media Access Control
MAN - Metropolitan Area Network
MEF - Metro Ethernet Forum
MFI - Multi-Frame Indicator
MLPPP - Multi Link Point-to-Point Protocol
NMS - Network Management System
MPLS - Multiprotocol Label Switching
MST - Member Status
MSTP - Multiservice Transporting Platform
NG-SDH - Next Generation SDH
OAM - Operation, Administration, and Maintenance
OTN - Optical Transport Network
OXC - Optical Cross-Connect
PCM - Pulse Coded Modulation
PCP - Priority Code Point
PDH - Plesiochronous Digital Hierarchy
PDU - Protocol Data Unit
PFI - Payload FCS Indicator
POH - Path Overhead
PPB-TE - Provider Backbone Bridge Traffic Engineering
PPP - Point-to-Point Protocol
PTI - Payload Type Identifier
QoS - Quality of Service
QSR - QoS Switch/Router
RAM - Random Access Memory
RS-Ack - Re-Sequence Acknowledge
SDH - Synchronous Digital Hierarchy
SF - Store-and-Forward Delay
SFD - Start-of-Frame-Delimiter
SLA - Service Level Agreement
SONET - Synchronous Optical Network
SQ - Sequence Indicator
STM - Synchronous Transport Module
TCI - Tag Control Information
tHEC - Type Header Error Control
TU - Tributary Unit
TUG - Tributary Unit Group
UNI - User-to-Network Interface
UPI - User Payload Identifier
VBR - Variable Bit Rate
VC - Virtual Container
VCat - Virtual Concatenation
VCG - Virtual Concatenation Group
VPLS - Virtual Private LAN Service
WAN - Wide Area Network
WDM - Wavelength Division Multiplexing

References

[1] R. M. Metcalfe and D. R. Boggs, "Ethernet: Distributed Packet Switching for Local Computer Networks," in *Communications of the ACM 19* (5),pp. 395-405, Jul. 1976.
[2] ITU-T, "Network Node Interface for the Synchronous Digital Hierarchy (SDH)," Recommendation G.707/Y.1322, Oct. 2000.
[3] ITU-T, "Generic Framing Procedure (GFP)," Recommendation G.7041/Y.1303, Dec. 2003.

[4] ITU-T, "Link Capacity Adjustment Scheme (LCAS) for Virtual Concatenated Signals," Recommendation G.7042/Y.1305, Feb. 2002.

[5] C. Spurgeon, "Ethernet, The Definitive Guide," O'Reilly, ISBN 1-56-592660-9, 2000.

[6] DEC, Xerox and Intel, "The Ethernet, a Local Area Network: Data Link Layer and Physical Layer Specifications," AA-K759B-TK, DEC, X3T51/80-50, XEROX, 1980.

[7] IEEE, "Carrier Sense Multiple Access with Collision Detection (CSMA/CD) Access Method and Physical Layer Specifications," IEEE Std 802.3-2008, December 26, 2008.

[8] M. Ali, G. Chiruvolu and A. Ge, "Traffic Engineering in Metro Ethernet," *IEEE Network*, pp. 10-17, Mar./Apr. 2005.

[9] W. Stallings, "Data and Computer Communications," Prentice Hall, 7th edition, ISBN 0-13-1000681-9, 2004.

[10] DARPA, "Internet Protocol," RFC 791, Sept. 1981.

[11] X. He, M. Zhu, and Q. Chu, "Transporting Metro Ethernet Services over Metropolitan Area Networks", in *Proceedings of the IEEE International Conference on Sensor Networks, Ubiquitous, and Trustworthy Computing*, 2006, pp. 178-185.

[12] V. Ramamurti, J. Siwko, G. Young, and M. Pepe, "Initial Implementations of Point-to-Point Ethernet over SONET/SDH Transport," *IEEE Communications Magazine*, pp. 64-70, Mar. 2004.

[13] IEEE, "Type 100BASE-T MAC parameters, Physical Layer, MAUs, and Repeater for 100 Mb/s Operation," IEEE Std 802.3u 1995 (Clauses 21 up to 30), Jun. 1995.

[14] A. Tanenbaum, "Computer Networks," Elsevier, 4th edition, ISBN 0-13-066102-3, 2003.

[15] IEEE, "Type 1000BASE-X MAC Parameters, Physical Layer, Repeater, and Management Parameters for 1000 Mb/s Operation," IEEE 802.3z-1998, 1998.

[16] IEEE, "Media Access Control (MAC) Parameters, Physical Layers, and Management Parameters for 10 Gb/s Operation," IEEE Std 802.3ae-2002, 2002.

[17] IEEE, "Amendment 1: Physical Layer and Management Parameters for 10 Gb/s Operation," Type 10GBASE-T, IEEE Std 802.3an-2006, 2006.

[18] F. Brockners, N. Finn and S. Phillips, "Metro Ethernet - deploying the extended campus using Ethernet technology," in *Proceedings of the 28th Annual IEEE International Conference on Local Computer Networks*, Oct. 2003, pp. 594-604.

[19] ITU-T, "B-ISDN ATM Layer Specification," Recommendation I.361, April 1991.

[20] L. Zier, W. Fisher and F. Brockners, "Ethernet-Based Public Communication Services: Challenge and Opportunity," *IEEE Communications Magazine*, pp. 88-95, Mar. 2004.

[21] A. Kasim et al., "Delivering Carrier Ethernet: Extending Ethernet Beyond the LAN," McGraw-Hill Osborne, ISBN 0-07-148747-6, 2007.

[22] R. Sanchez, L. Raptis, K. Vaxevanakis, "Ethernet as a Carrier Grade Technology: Developments and Innovations," *IEEE Communications Magazine*, pp. 88-94, Sep. 2008.

[23] A. Reid, P. Willis, I. Hawkings and C. Bilton, "Carrier Ethernet," *IEEE Communications Magazine*, pp. 96-103, Sep. 2008.

[24] MEF, "Carrier Ethernet Services Overview," Metro Ethernet Forum, 2008.

[25] H. Ohta, "Standardization Status of Carrier- Class Ethernet," *NTT Technical Review*, 2008.

[26] ITU-T, "Ethernet over Transport: Ethernet services framework," Recommendation G.8011/Y.1307, Aug. 2004.

[27] MEF, "Metro Ethernet Services Definitions Phase 2," Metro Ethernet Forum Technical Specification, April 2008.

[28] M. Lasserre and V. Kompella, "Virtual Private LAN Service (VPLS) Using Label Distribution Protocol (LDP) Signaling," Internet Engineering Task Force, RFC 4762, January 2007.

[29] IEEE, "Virtual Bridged Local Area Networks," IEEE Std 802.1Q-2005, 2005.

[30] R. Seifert and J. Edwards, "The All-New Switch Book: The Complete Guide to LAN Switching Technology," Wiley-India, 2nd edition, ISBN 0-47-028715-2, 2008.

[31] IEEE, "Virtual Bridged Local Area Networks Amendment 4: Provider Bridges," IEEE 802.1ad 2005, 2005.

[32] IEEE, "Virtual Bridged Local Area Networks Amendment 7: Provider Backbone Bridges," IEEE Std 802.1ah-2008, 2008.

[33] X. Xiao, "Technical, Commercial and Regulatory Challenges of QoS: An Internet Service Model Perspective," Morgan Kaufamann, ISBN 0-12-373693-5, 2008.

[34] IEEE, "Media Access Control (MAC) Bridges," IEEE Std 802.1D-2004, 2004.

[35] ITU-T,"A QoS control architecture for Ethernet-based IP access networks," Recommendation Y.2112, June 2007.

[36] MEF, "Ethernet Services Attributes Phase 2," Metro Ethernet Forum Technical Specification, November 2006.

[37] IEEE, "Virtual Bridged Local Area Networks Amendment: Provider Backbone Bridge Traffic Engineering," IEEE Draft Std 802.1Qay, 2009.

[38] IEEE, "Ethernet in the First Mile," IEEE Std 802.3ah-2004, 2004.

[39] B. Mukherjee, "Optical WDM Networks," Springer Verlag, ISBN 0-38-729055-9, 2006.

[40] IEEE, "Virtual Bridged Local Area Networks Amendment 5: Connectivity Fault Management," IEEE Std 802.1ag-2007, 2007.

[41] ITU-T, "OAM Functions and Mechanisms for Ethernet based Networks," Recommendation Y.1731, Feb. 2008.

[42] ITU-T, "Ethernet Protection Switching," Recommendation G.8031/Y.1342, Jun. 2006.

[43] ITU-T, "General Hierarchy Bit Rates," Recommendation G.702, 1988.

[44] ISO/IEC, "High-Level Data Link Control (HDLC) Procedures," Standard 13239:2002, 2002.

[45] ITU-T, "Management aspects of synchronous digital hierarchy (SDH) transport network elements," Recommendation G.784, Mar. 2008.

[46] G. Bernstein, B. Rajagopalan and D. Saha, "Optical Network Control: Architecture, Protocols, and Standards," Addison-Wesley, ISBN 0-20-175301-4, 2003.

[47] J. Manchester, J. Anderson, B. Doshi and S. Dravida, "IP over SONET," *IEEE Communications Magazine*, pp. 136-142, May 1998.

[48] P. Bonenfant and A. Rodrigues-Moral, "Framing Techniques for IP over Fiber," *IEEE Network*, pp. 12-18, Jul./Aug. 2001.

[49] H. Hernandez-Valencia, M. Scholten, and Z. Zhu, "The Generic Framing Procedure (GFP): An Overview," *IEEE Communications Magazine*, pp. 63-71, May 2002.

[50] M. Scholten, Z. Zhu, H. Hernandez-Valencia, and J. Hawkins, "Data Transport Applications Using GFP," *IEEE Communications Magazine*, pp. 96-103, May 2002.

[51] X. Li, D. Jin., and L. Zeng, "Encapsulation and Rate Adaptation for Ethernet over SDH," in *IEEE International Conference on Communications, Circuits and Systems and West Sino Expositions*, 2002, pp. 1301-05.

[52] ITU-T, "IP over SDH using LAPS," March 2001, Recommendation X.85/Y.1321.

[53] A. Malis and W. Simpson, "PPP over SONET/SDH ," Internet Engineering Task Force, RFC 2615, June 1999.

[54] ITU-T, "Ethernet over LAPS," February 2001, Recommendation X.86/Y.1323.

[55] ITU-T,"Interface for the Optical Transport Network (OTN)," Recommendation G.709/Y.1331, 2003.

[56] E. Rosen, A. Viswanathan, and R. Callon, "Multiprotocol Label Switching Architecture," Internet Engineering Task Force, RFC 3031, Jan. 2001.

[57] W. Simpson, "The Point-to-Point Protocol (PPP)," Internet Engineering Task Force, RFC 1661, July 1994.

[58] Ramaswami, R. and Sivarajan, K. N.,"Optical networks: A Practical Perspective," Morgan Kaufmann, ISBN: 1-55-860655-6, 2002.

[59] P. Bonenfant and A. Rodrigues-Moral, "Generic Framing Procedure (GFP): The Catalyst for Efficient Data over Transport," *IEEE Communications Magazine*, pp. 72-79, May 2002.

[60] S. S. Gorshe and T. Wilson, "Transparent Generic Framing Procedure (GFP): A Protocol for Efficient Transport of Block-Coded Data through SONET/SDH Networks," *IEEE Communications Magazine*, pp. 88-95, May 2002.

[61] M. N. Ellanti, S. S. Gorshe, L. G. Raman, and W. D. Grover, " Next Generation Transport Networks: Data, Management, and Control Planes," Springer, 1st Edition, ISBN 0-38-724067-5, 2005.

[62] ANSI, "Synchronous Optical Network (SONET) - Basic Description Including Multiplex Structure, Rates, and Formats," T1.105-2001, 2001.

[63] ITU-T, "Characteristics of Synchronous Digital Hierarchy (SDH) Equipment Functional Blocks," Recommendation G.783, Mar. 2006.

[64] G. Bernstein, D. Caviglia, R. Rabbat, and H. V. Helvoort, "VCAT-LCAS in a Clamshell," *IEEE Communications Magazine*, pp. 34-36, May 2006.

[65] Sklower, K., Lloyd, B., McGregor, G., Carr, D., and T. Coradetti, "The PPP Multilink Protocol (MP)", RFC 1990, Aug. 1996.

[66] ITU-T, "Virtual Concatenation of Plesiochronous Digital Hierarchy (PDH) Signals ," Recommendation G.7043/Y.1343, Jul. 2004.

[67] H. V. Helvoort, "Next Generation SDH/SONET: Evolution or Revolution," Wiley, 1st Edition, ISBN 0-47-009120-7, 2005.

[68] G. Garg and S. Paul, "Managing Differential Delay in SONET Architectures," Commsdesign, White Paper, 2002.

[69] G. Shi, Q. Wang, Z. Liu, and L. Zeng, "SDH Virtual Concatenation Technique Used in Ethernet Data Transport," in *IEEE International Conference on Communications, Circuits and Systems and West Sino Expositions*, 2002, pp. 1784-1787.
[70] G. Barlow, "Traffic Delay in Ethernet over SONET/SDH," Innocor Ltd., White Paper, 2004.
[71] S. Bradner and J. McQuaid, "Benchmarking Methodology for Network Interconnect Devices," Internet Engineering Task Force, RFC 2544, March 1999.
[72] L. H. Dahai, "Performance Comparison of GFP and LAPS in Application of Data-transport," in *Proceedings 2005 International Conference on Communications, Circuits and Systems*, 2005, pp. 618-21.
[73] S. Gunreben and C. M. Gauger, "Dynamic Bandwidth Adaptation in NG SDH/WDM Transport Networks using LCAS," in *Proceedings of the 10th European Conference on Networks and Optical Communications*, 2005.
[74] L. Ge and T. Yoshimura, "Design and Implementation of an EoS Chip," in *6th International Conference On ASICON*, 2005, pp. 300-03.
[75] J. Kuri, M. Gagnaire, N. Puech, O. Audouin, and R. Douville, "On the Resource Efficiency of Virtual Concatenation in Next-Generation SDH Networks," in *2nd International Conference on Broadband Networks*, BroadNets, October 2005, pp. 78-86.
[76] H. J. Kim, S. Myong, H. H. Hong, J. H. Lee, and J. S. Kim, "The Role of Ethernet over SDH in QoS Switch/Router," in *8th International Conference in Advanced Communication Technology*, 2006, pp. 985-990.
[77] H. Tzeng and C. Chiu, "A Flexible Cross Connect LCAS for Bandwidth Maximization in 2.5G EoS," in *Fifth IEEE International Symposium on Network Computing and Applications*, 2006, pp. 243-246.
[78] C. Wentao, J. Depeng, and L. Zeng, "Performance Analysis of Two Ethernet over E1 Schemes," *Tsinghua Science & Technology Magazine*, pp. 70-76, Feb. 2007.
[79] ITU-T, "Synchronous Frame Structures Used at 1544, 6312, 2048, 8448 and 44 736 kbit/s Hierarchical Levels," Recommendation G.704, Oct. 1998.
[80] telecomasia.net, "Teething problems for Carrier Ethernet," Available online at http://www.telecomasia.net/content/eu-telecom-ministers-thumb-down-plan-regulatory-body in July 2010.
[81] IETF, "GMPLS Controlled Ethernet Label Switching," GELS Working Group, Available online at http://www.ietf.org/proceedings/64/gels.html in July 2010.

Antonio Marcos Alberti received the degree in Electrical Engineering from Santa Maria Federal University (UFSM), Santa Maria, RS, Brazil, in 1986, and the M.Sc. and Ph.D. degrees in Electrical Engineering from Campinas State University (Unicamp), Campinas, SP, Brazil, in 1998 and 2003, respectively. In February 2004 he joined the Instituto Nacional de Telecomunicações (INATEL), as an Adjunct Professor. He has experience in teaching more than 8 post-graduation disciplines, including Analysis and Performance Evaluation of Communication Networks, Optimization Methods Applied to Telecommunications and Convergent Networks. He is a member of the editorial board of the INATEL telecommunications magazine. He was member of the technical committee of Globecom, TEMU, ICDT and ANSS conferences. In 2010, wrote a book chapter entitled "Future Network Architectures: Technological Challenges and Trends" that discusses technological requirements, challenges and trends towards future network architectures. His main working area is communication networks, where he has expertise in project, modeling, simulation, performance evaluation and optimization of such networks. His current interests include future networks design, cognitive and autonomic networks, indirection resolution, entities identification, virtualization and future enabling technologies.

Roulien Fernandes received the Electrical Engineering degree from Universidade São Judas Tadeu (USJT) in 1984. From 1985 up to 1992, he joined the Universidade São Judas Tadeu as a teacher. From 1986 up to 1989, he coordinated deployments of automatized systems for process control and industrial automation at Toledo do Brasil enterprise.Since 1989, he works on telecommunications area at Laboratório de Qualificação de Produtos from Telefônica do Brasil. His activities range from new products technical evaluation, development of prospecting studies and evaluation of new technologies to be employed by Telefonica do Brasil S.A. He is also responsible by the coordination of teams at testing laboratories. The focus is on transmission, external and access networks, aimed to qualify and homologate equipments. In 2003, he wrote the paper "Characterisation of Office main distribution frame for ADSL-DMT services", published at IEE. His main area of work is optical transport networks, acting in its evolution since the deployment of the SDH, DWDM, and later evolving into the ASON-G-MPLS technology. More recently, he is working in the evolution to photonic networks, developing optical control planes combined with electrical G-MPLS. Such approach uses ODU (Optical Digital Unit)-based OTN switch technology as well as high-speed optical interfaces (100Gbps).

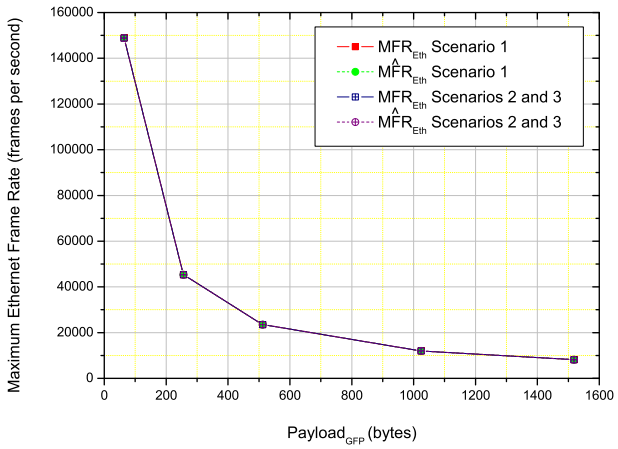

Fig. 6. Measured and calculated maximum Ethernet frame (+gaps) rates per second.

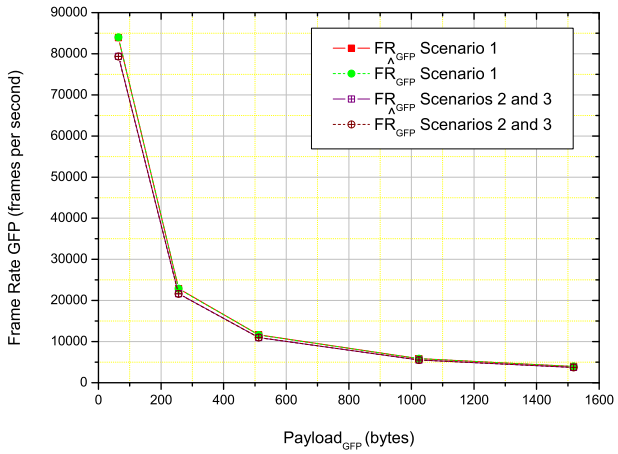

Fig. 7. Measured and calculated GFP frame rates per second passed to complete a VC-n-Xv.

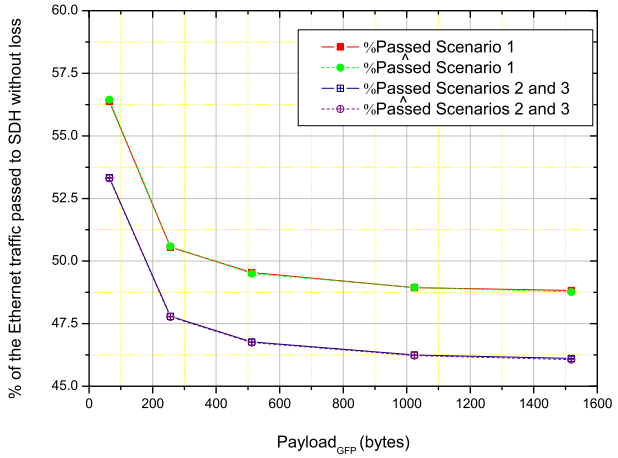

Fig. 8. Measured and calculated percentages of Ethernet traffic passed without loss to SDH.

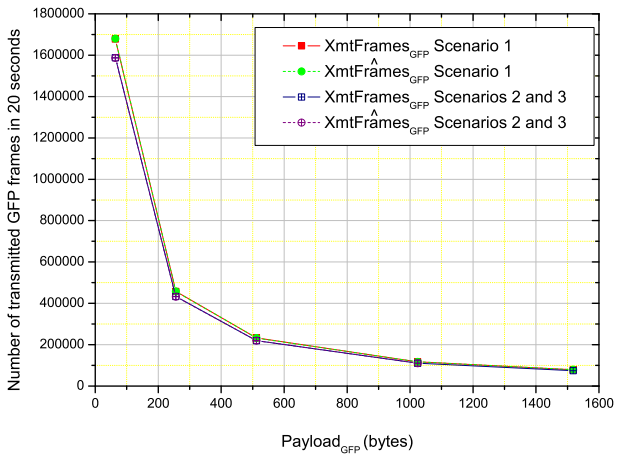

Fig. 9. Measured and calculated numbers of GFP frames transmitted in 20 seconds.

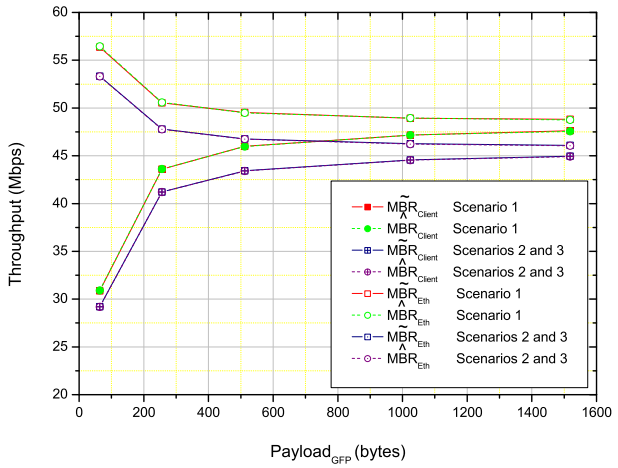

Fig. 10. Semi-analytical and analytical throughputs available for Ethernet clients and Megabit rates of Ethernet traffic.

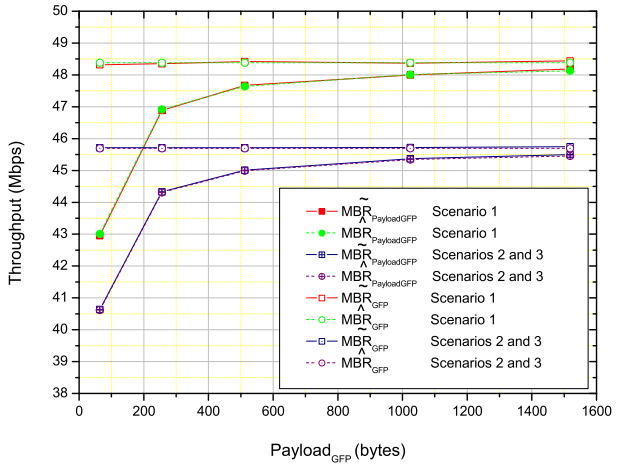

Fig. 11. Semi-analytical and analytical Megabit rates of GFP payload and GFP frames.

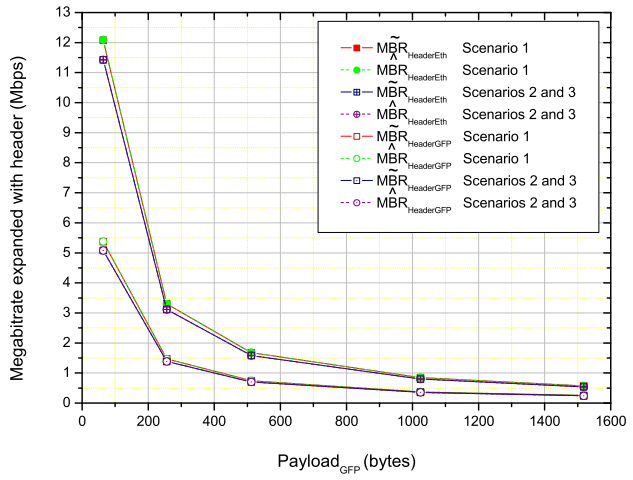

Fig. 12. Semi-analytical and analytical Megabit rates spent on Ethernet and GFP headers.

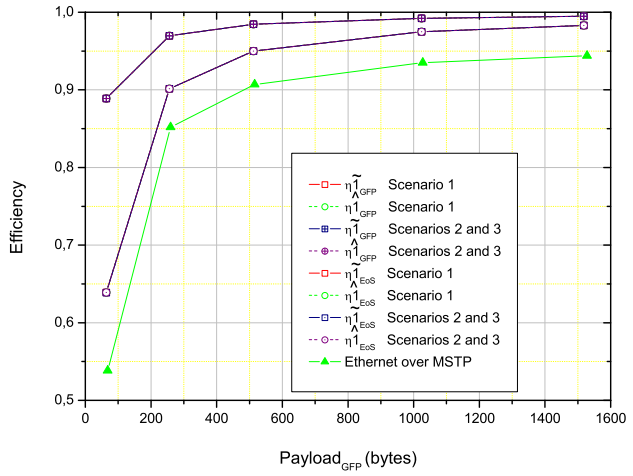

Fig. 13. Semi-analytical and analytical efficiencies of GFP and EoS encapsulation. The Ethernet over *Multiservice Transporting Platform* (MSTP) curve is from reference He et al. [11].

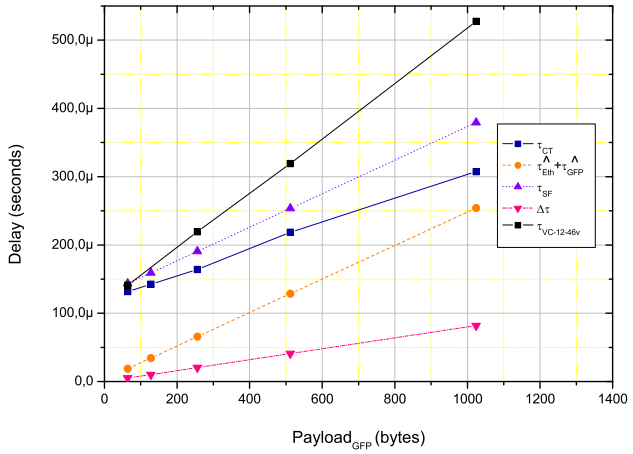

Fig. 14. Measured and analytical delay results in Scenario 1.

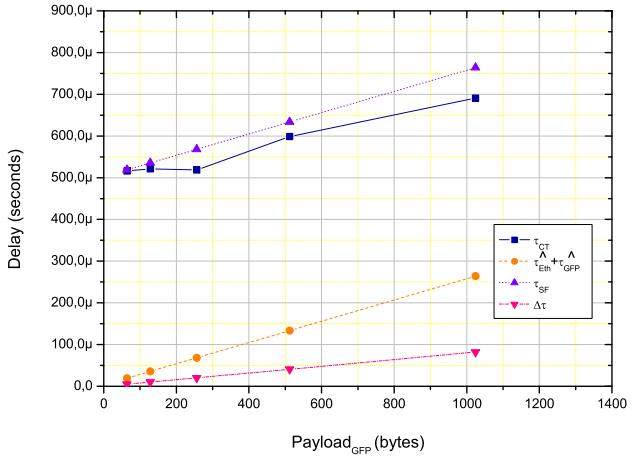

Fig. 15. Measured delay in Scenario 2.

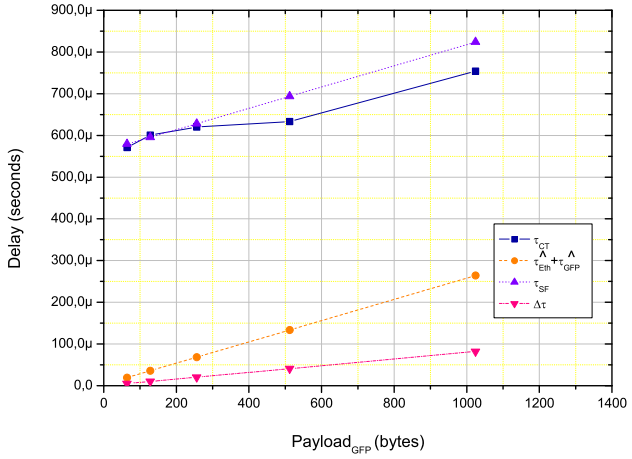

Fig. 16. Measured delay in Scenario 3.

TABLE I

MEASURED RESULTS FOR SCENARIO 1: ETHERNET/GFP/VC-3-1V.

$Payload_{GFP}$ (bytes)	64	256	512	1024	1518
MFR_{Eth} (frames+gaps/sec.)	148810	45290	23496	11973	8127
FR_{GFP} (frames/sec.)	83893	22894	11639	5859	3968
$\%Passed$	56.38	50.55	49.54	48.94	48.82
$XmtFrames_{GFP}$ (# of frames)	1677852	457875	232774	117178	79365
$RcvFrames_{GFP}$ (# of frames)	1677852	457875	232774	117178	79365
$RcvPayloadBytes_{GFP}$ (bytes)	107382528	117216000	119180288	119990272	120476070

TABLE II

CALCULATED RESULTS FOR SCENARIO 1.

$Payload_{GFP}$ (bytes)	64	256	512	1024	1518
$\hat{MFR}_{Eth}$ (frames+gaps/sec.)	148809.52	45289.85	23496.24	11973.18	8127.44
$\hat{FR}_{GFP}$ (frames/sec.)	84000	22909.09	11630.77	5860.46	3963.30
$\hat{\%Passed}$	56.448	50.583	49.501	48.947	48.764
$\hat{XmtFrames}_{GFP}$ (# of frames)	1680000	458181.82	232615.38	117209.30	79266.05
$\hat{RcvFrames}_{GFP}$ (# of frames)	1680000	458181.82	232615.38	117209.30	79266.05
$\hat{RcvPayloadBytes}_{GFP}$ (bytes)	107520000	117294545	119099077	120022326	120325872
$\hat{MBR}_{Client}$ (Mbit/s)	30.9120	43.6189091	45.9648000	47.1650233	47.5596330
$\hat{MBR}_{Eth}$ (Mbit/s)	56.4480	50.5832727	49.5005538	48.9466047	48.7644771
$\hat{MBR}_{PayloadGFP}$ (Mbit/s)	43.0080	46.9178182	47.6396308	48.0089302	48.1303486
$\hat{MBR}_{GFP}$ (Mbit/s)	48.3840	48.3840	48.3840	48.3840	48.3840
$\hat{MBR}_{EthHeader}$ (Mbit/s)	12.0960	3.2989091	1.6748308	0.8439070	0.5707156
$\hat{MBR}_{GFPHeader}$ (Mbit/s)	5.3760	1.4661818	0.7443692	0.3750698	0.2536514
$\hat{\eta 1}_{GFP}$	0.8889	0.9697	0.9846	0.9922	0.9948
$\hat{\eta 1}_{EoS}$	0.6389	0.9015	0.95	0.9748	0.983

TABLE III

SEMI-ANALYTICAL RESULTS FOR SCENARIO 1.

$Payload_{GFP}$ (bytes)	64	256	512	1024	1518
$\tilde{MBR}_{Client}$ (Mbit/s)	30.872624	43.590176	45.997328	47.153232	47.616
$\tilde{MBR}_{Eth}$ (Mbit/s)	56.376096	50.549952	49.535584	48.934368	48.822272
$\tilde{MBR}_{PayloadGFP}$ (Mbit/s)	42.953216	46.886912	47.673344	47.996928	48.187392
$\tilde{MBR}_{GFP}$ (Mbit/s)	48.322368	48.352128	48.41824	48.371904	48.441344
$\tilde{MBR}_{EthHeader}$ (Mbit/s)	12.080592	3.296736	1.676016	0.843696	0.571392
$\tilde{MBR}_{GFPHeader}$ (Mbit/s)	5.37	1.47	0.74	0.37	0.25
$\tilde{\eta 1}_{GFP}$	0.8889	0.9697	0.9846	0.9922	0.9948
$\tilde{\eta 1}_{EoS}$	0.6389	0.9015	0.9500	0.9748	0.9829

TABLE IV

MEASURED RESULTS FOR SCENARIOS 2 AND 3: ETHERNET/GFP/VC-12-21V AND ETHERNET/GFP/(VC-12-10V+VC-12-11V).

$Payload_{GFP}$ (bytes)	64	256	512	1024	1518
MFR_{Eth} (frames+gaps/sec.)	148810	45290	23496	11973	8127
FR_{GFP} (frames/sec.)	79365	21645	10989	5538	3747
$\%Passed$	53.33	47.79	46.77	46.25	46.11
$XmtFrames_{GFP}$ (# of frames)	1587301	432900	219780	110766	74940
$RcvFrames_{GFP}$ (# of frames)	1587301	432900	219780	110766	74940
$RcvPayloadBytes_{GFP}$ (bytes)	101587264	110822400	112527360	113424284	113758920

TABLE V

ANALYTICAL EXPRESSIONS RESULTS FOR SCENARIOS 2 AND 3.

$Payload_{GFP}$ (bytes)	64	256	512	1024	1518
$\hat{MFR}_{Eth}$ (frames+gaps/sec.)	148809.5	45289.8	23496.2	11973.2	8127.4
$\hat{FR}_{GFP}$ (frames/sec.)	79333.3	21636.3	10984.6	5534.9	3743.1
$\hat{\%Passed}$	53.31	47.77	46.75	46.23	46.06
$\hat{XmtFrames}_{GFP}$ (# of frames)	1586666.6	432727.3	219692.3	110697.7	74862.4
$\hat{RcvFrames}_{GFP}$ (# of frames)	1586666.6	432727.3	219692.3	110697.7	74862.4
$\hat{RcvPayloadBytes}_{GFP}$ (bytes)	101546666	110778181	112482461	113354418	113641100
$\hat{MBR}_{Client}$ (Mbit/s)	29.1947	41.1956	43.4112	44.5447	44.9174
$\hat{MBR}_{Eth}$ (Mbit/s)	53.312	47.7731	46.7505	46.2273	46.0553
$\hat{MBR}_{PayloadGFP}$ (Mbit/s)	40.6187	44.3113	44.993	45.3418	45.4564
$\hat{MBR}_{GFP}$ (Mbit/s)	45.696	45.696	45.696	45.696	45.696
$\hat{MBR}_{EthHeader}$ (Mbit/s)	11.424	3.1156	1.5818	0.797	0.539
$\hat{MBR}_{GFPHeader}$ (Mbit/s)	5.0773	1.3847	0.703	0.3542	0.2396
$\hat{\eta 1}_{GFP}$	0.8889	0.9697	0.9846	0.9922	0.9948
$\hat{\eta 1}_{EoS}$	0.6389	0.9015	0.95	0.9748	0.983

TABLE VI

SEMI-ANALYTICAL RESULTS FOR SCENARIOS 2 AND 3.

$Payload_{GFP}$ (bytes)	64	256	512	1024	1518
$\tilde{MBR}_{Client}$ (Mbit/s)	29.20632	41.21208	43.428528	44.569824	44.964
$\tilde{MBR}_{Eth}$ (Mbit/s)	53.33328	47.79216	46.769184	46.253376	46.103088
$\tilde{MBR}_{PayloadGFP}$ (Mbit/s)	40.63488	44.32896	45.010944	45.367296	45.503568
$\tilde{MBR}_{GFP}$ (Mbit/s)	45.71424	45.71424	45.71424	45.721728	45.743376
$\tilde{MBR}_{EthHeader}$ (Mbit/s)	11.42856	3.11688	1.582416	0.797472	0.539568
$\tilde{MBR}_{GFPHeader}$ (Mbit/s)	5.07936	1.38528	0.703296	0.354432	0.239808
$\tilde{\eta 1}_{GFP}$	0.8889	0.9697	0.9846	0.9922	0.9947
$\tilde{\eta 1}_{EoS}$	0.6388	0.9015	0.9500	0.9748	0.9830

TABLE VII

LINK TEAR DOWN WITH LCAS ACTIVE FOR $Payload_{GFP}$ EQUAL TO 512 BYTES.

$Link(B-C)Status$	On	Off	On
MFR_{Eth} (frames+gaps/sec.)	23496	23496	23496
FR_{GFP} (frames/sec.)	10999	5752	10999
$\%Passed$	46.81	24.48	46.81
$XmtFrames_{GFP}$ (# of frames)	219973	115048	219973
$RcvFrames_{GFP}$ (# of frames)	219973	115048	219973
$RcvPayloadBytes_{GFP}$ (bytes)	112626176	58904576	112626176
$\tilde{MBR}_{Client}$ (Mbit/s)	43.468048	22.731904	43.468048
$\tilde{MBR}_{PayloadGFP}$ (Mbit/s)	45.051904	23.560192	45.051904
$\tilde{MBR}_{GFP}$ (Mbit/s)	45.71424	23.92832	45.71424
$\tilde{MBR}_{EthHeader}$ (Mbit/s)	1.583856	0.828288	1.583856
$\tilde{MBR}_{GFPHeader}$ (Mbit/s)	0.703936	0.368128	0.703936
$\tilde{\eta 1}_{GFP}$	0.9846	0.9846	0.9846
$\tilde{\eta 1}_{EoS}$	0.9499	0.9499	0.9499

TABLE VIII

LCAS DECREASING AND INCREASING THE NUMBER OF VIRTUAL CONCATENATED VCS FOR $Payload_{GFP}$ EQUAL TO 512 BYTES.

$Link(B-C)Status$	On	Off	On
FR_{Eth} (frames+gaps/sec.)	23496	23496	23496
FR_{GFP} (frames/sec.)	10989	10465	10989
$\%Passed$	46.77	44.54	46.77
$XmtFrames_{GFP}$ (# of frames)	219780	209292	219780
$RcvFrames_{GFP}$ (# of frames)	219780	209292	219780
$RcvPayloadBytes_{GFP}$ (bytes)	112527360	107157504	112527360
MBR_{Client} (Mbit/s)	43.428528	41.35768	43.428528
$MBR_{PayloadGFP}$ (Mbit/s)	45.010944	42.86464	45.010944
MBR_{GFP} (Mbit/s)	45.71424	43.5344	45.71424
$MBR_{EthHeader}$ (Mbit/s)	1.583856	0.828288	1.583856
$MBR_{GFPHeader}$ (Mbit/s)	0.703936	0.368128	0.703936
$\eta 1_{GFP}$	0.9846	0.9846	0.9846
$\eta 1_{EoS}$	0.95	0.95	0.95

TABLE IX

SUBMITTED ETHERNET FRAMES (+GAPS) PER SECOND IN DELAY EXPERIMENTS TO COMPLETE THE TESTED BIT RATES.

$Payload_{GFP}$ (bytes)	64	128	256	512	1024
FR_{Eth} @30 Mbit/s	44643	25355	13587	7048	3591

TABLE X

PORT-PAIR LATENCY FOR ETHERNET/GFP/VC-3-1V.

$Payload_{GFP}$ (bytes)		64	128	256	512	1024
30 Mbit/s	$\tau_{CT}(\mu s)$	136.9	152.8	184.6	259.6	389.4
	$\tau_{SF}(\mu s)$	131.8	142.6	164.2	218.7	307.5
$\Delta\tau(\mu s)$		5.1	10.2	20.4	40.9	81.9

TABLE XI

PORT-PAIR LATENCY FOR ETHERNET/GFP/VC-12-21V.

$Payload_{GFP}$ (bytes)		64	128	256	512	1024
30 Mbit/s	$\tau_{CT}(\mu s)$	521.3	531.7	539	639.6	772.9
	$\tau_{SF}(\mu s)$	516.2	521.5	518.6	598.7	691
$\Delta\tau(\mu s)$		5.1	10.2	20.4	40.9	81.9

TABLE XII

PORT-PAIR LATENCY FOR ETHERNET/GFP/(VC-12-10V+VC-12-11V).

$Payload_{GFP}$ (bytes)		64	128	256	512	1024
30 Mbit/s	$\tau_{CT}(\mu s)$	576	610.9	640.7	674.3	836
	$\tau_{SF}(\mu s)$	570.9	600.7	620.3	633.4	754.1
$\Delta\tau(\mu s)$		5.1	10.2	20.4	40.9	81.9